UCRL-11901

University of California

Ernest O. Lawrence Radiation Laboratory

TWO-WEEK LOAN COPY

This is a Library Circulating Copy which may be borrowed for two weeks. For a personal retention copy, call Tech. Info. Division, Ext. 5545

I. SIMILARITY PRINCIPLE AND ISOTOPE EFFECT IN SUPERCONDUCTING INDIUM
II. LOW-TEMPERATURE HEAT CAPACITY OF NIOBIUM

Berkeley, California

DISCLAIMER

This document was prepared as an account of work sponsored by the United States Government. While this document is believed to contain correct information, neither the United States Government nor any agency thereof, nor the Regents of the University of California, nor any of their employees, makes any warranty, express or implied, or assumes any legal responsibility for the accuracy, completeness, or usefulness of any information, apparatus, product, or process disclosed, or represents that its use would not infringe privately owned rights. Reference herein to any specific commercial product, process, or service by its trade name, trademark, manufacturer, or otherwise, does not necessarily constitute or imply its endorsement, recommendation, or favoring by the United States Government or any agency thereof, or the Regents of the University of California. The views and opinions of authors expressed herein do not necessarily state or reflect those of the United States Government or any agency thereof or the Regents of the University of California.

UCRL-11901

UNIVERSITY OF CALIFORNIA

Lawrence Radiation Laboratory
Berkeley, California

AEC Contract W-7405-eng-48

I. SIMILARITY PRINCIPLE AND ISOTOPE EFFECT IN SUPERCONDUCTING INDIUM

II. LOW-TEMPERATURE HEAT CAPACITY OF NIOBIUM

Nail Mehmet Senozan

(Ph.D. Thesis)

January 1965

4. Analysis of Data 68

A. Normal State 68

B. Superconducting State 69

C. Mixed State 71

D. Comparison with Other Measurements 71

5. Discussion 76

Acknowledgments 82

Part II - References 83

Part II - Figure Captions 86

Part II - Figures 87

I. SIMILARITY PRINCIPLE AND ISOTOPE EFFECT IN SUPERCONDUCTING INDIUM
II. LOW TEMPERATURE HEAT CAPACITY OF NIOBIUM

Nail Mehmet Senozan

Inorganic Materials Research Division, Lawrence Radiation Laboratory,
Department of Chemistry, University of California,
Berkeley, California

ABSTRACT

PART I

Theories predict that the critical field curves of the isotopes of a superconductor are similar if the lattice contributions, $C_{\ell n}$ and $C_{\ell s}$, to the normal and superconducting state heat capacities of this superconductor are the same. Recent measurements have indicated that the low temperature heat capacity of indium is anomalous; $C_{\ell s}$ is about 15% smaller than $C_{\ell n}$. In order to see whether this anomaly is reflected in the critical fields as the theories predict we undertook critical field measurements between 1°K and the transition temperature 3.4°K, on five isotopically enriched indium specimens. It was found that the critical fields are similar within one part in 600 and, furthermore, that the isotope effect is present - the transition temperature, T_c, being dependent on the isotopic mass, M, as $T_c \propto M^{-\frac{1}{2}}$.

PART II

As an extension of the work described in Part I, we wanted to investigate whether the indium anomaly is unique or whether it is common to other superconductors. Niobium was chosen because its high transition temperature, 9.2°K, allows one to work at very low reduced temperatures where, according to the BCS theory, the electronic contribution to the heat

capacity of the superconducting state becomes negligible and a comparison of the lattice terms is possible.

Using a He^3 calorimeter measurements between .25° and 25°K were made on a single crystalline specimen of niobium in which the total impurities were less than 80 parts per million. It was found that at low temperatures ($T \lesssim 5°K$) the normal state heat capacity, C_n, is best represented as

$$C_n = 7.85 + 0.0915\ T^3 + 0.0010\ T^5 \text{ millijoules/mole degree}$$

The behavior of the superconducting state heat capacity, C_s, is striking: At very low temperatures it does not approach $C_{\ell n}$, the normal state lattice heat capacity; in fact, it does not have a T^3 dependence. The results are best understood by assuming equal lattice contributions in the normal and superconducting state heat capacities. The superconducting state heat capacity can then be written as

$$C_s = C_{es} + 0.0915\ T^3 + 0.0010\ T^5 \text{ millijoules/mole degree}$$

where C_{es} is best represented by

$$C_{es} = (7.85\ T_c)(7.85\ e^{-1.49\frac{T_c}{T}} + 2.6\text{X}10^{-3}\ e^{-0.053\frac{T_c}{T}}) \text{ millijoules/mole degree}$$

This suggests that the energy gap in niobium is very strongly anisotropic.

I. SIMILARITY PRINCIPLE AND ISOTOPE EFFECT IN SUPERCONDUCTING INDIUM

I. Introduction

Until recently in analyzing low temperature specific heat measurements on superconductors it has been customary to assume equal lattice contributions for the normal and the superconducting phases. This assumption is consistent with currently accepted theories and also with a number of experiments. X-ray crystallography, for example, reveals that the lattice structure is the same for both states, and sound velocity measurements indicate a difference of only one part in 10,000 between the elastic constants of the normal and the superconducting states. For indium, for example, Chandrasekhar and Rayne[1] found that at 0°K the difference is less than one part in 10,000. For other metals[2] it has been established that this difference is even less.

What seemed to be a violation of this common assumption came in 1960, when C. A. Bryant and P. H. Keesom[3] published their results on the heat capacity of indium. Their measurements, which extended from 4°K to 0.35°K, revealed that below 0.8°K the total superconducting state heat capacity was less than that of the normal state lattice term alone. This fact was later confirmed by H. R. O'Neal[4,5,6] in his measurements between 0.1°K and 4°K.

Stimulated by these specific heat results and by the theoretical arguments of P. M. Marcus and E. Maxwell[7] and of G. V. Chester,[8] that relate the lattice heat capacity to the dependence of critical field on isotopic mass, we decided to undertake critical field measurements on isotopically enriched indium samples. As we shall point out in detail in Section 3, Marcus and Maxwell, after making certain assumptions, showed

that the equality of the lattice specific heats for the normal and superconducting states necessitates the validity of the similarity principle; that is, the critical field curves expressed in terms of the reduced variables $h = H_c/H_o$ and $t = T/T_c$ are identical for the different isotopes. Hc is the critical magnetic field, H_o is its value at temperature T = 0, and Tc is the zero field transition temperature. Chester, reasoning in the reverse direction, argued that the similarity principle implies the equality of the lattice heat capacities. Hence, for indium where the lattice specific heats are not equal one might expect the similarity principle to break down.

An important by-product of our critical field measurements on the indium isotopes was the establishment of the isotope effect. The isotope effect, which was first discovered for mercury by E. Maxwell[9] and Reynolds et al.[10] in 1950, can be described by the relation

$$M^{\alpha}\, Tc = \text{constant}$$

where M is the average isotopic mass, Tc the superconducting transition temperature, and α a constant. Shortly after the discovery of the isotope effect in mercury, studies were made on tin,[11,12,13] thallium,[14] and lead.[13,15] All these metals did show an isotope effect and the value of α for all except lead was found to be about +0.5. For lead α was first thought to be about 0.75, but more careful measurement by D. E. Mapother and coworkers[16,17] showed that it also was about +0.5.

The discovery of the isotope effect had a profound impact on the theoretical development of superconductivity. Here was a phenomenon clearly indicating a connection between the lattice vibrations (phonons) and the occurance of superconductivity. Such a connection had already

been suggested by H. Fröhlich in his attempt to construct a theory of superconductivity on the basis of phonon-electron interaction,[18] and this idea was eventually developed in the now celebrated theory of Bardeen, Cooper, and Schrieffer.[19]

In the theory of Bardeen, Cooper, and Schrieffer (BCS), $\alpha = +0.5$. This result was not seriously questioned until Geballe and co-workers[20] reported that ruthenium showed no isotope effect, and suggested that this implied a mechanism other than an electron-phonon interaction. A close examination of the BCS theory, however, reveals that the prediction of the isotope effect with $\alpha = 0.5$ has been "induced" into the theory by an arbitrary choice of the range of interaction between electrons.

On one hand the arbitrary nature of the BCS theory in predicting an isotope effect with $\alpha = +0.5$ and, on the other, the absence of this effect in ruthenium[20] and osmium,[21] makes it interesting to establish the α values for the yet untried elements. More recently isotope effect measurements have been made on Zn,[21] Mo,[22] Mo_3Ir[22] and Nb_3Sn[23] with the α values about +1/2, +1/3, +1/3 and 0.08 respectively. Indium with its abnormal heat capacity behavior is thus an interesting candidate for the study of critical field as a function of isotopic mass in two respects.

The results of our critical field measurements together with our findings about the isotope effect will be given in Sec. 3. Section 2 is devoted to the experimental aspects, and the reader uninterested in these problems may proceed directly to Sec. 3.

2. Description of Apparatus and Measurements

Essentially, the determination of the critical field of a specimen consists of measuring its magnetic permeability μ as a function of an applied magnetic field at some constant temperature T. As the magnetic field transforms the sample into the normal state μ rises, and when superconductivity is completely quenched it becomes equal to that of the normal state. Plotting μ versus the magnetic field H, one can determine the critical field H_c corresponding to T.

A schematic drawing of the circuit used in the permeability measurements is shown in Fig. 1. An alternating current of 23 cycle per second and 25 ma was passed through the primary coil P inducing signals in the two secondaries S and B. S containing the sample and B acting as a blank were connected in the opposite sense. Thus, had the sample not been present and had there been no resistive losses, the induced emf's in these two secondary coils would have cancelled each other and no signal would have been observed on the oscilloscope. The presence of a sample causes the inductive coupling between P and S to be different from that between P and B. Different emf's are then induced and a signal is observed on the oscilloscope. In order to achieve the null condition again a certain amount of inductance must be added to the circuit. This is done by means of the mutual inductance box M, which is similar to one described by Erickson, Roberts and Dobbs.[24] In general adding some inductance alone will not be sufficient to achieve the null condition because of the losses that occur in the specimen and contribute a secondary voltage that is in phase with the primary current. In order to establish a null condition then, we not only have to change M, but we also have to add a resistive component of voltage to the secondary circuit. The variable resistance R

in the circuit of Fig. 1 is for this purpose.

To determine the critical field of a sample at some temperature T, the temperature was regulated at the desired value and the null condition was established by making appropriate changes of inductance and transfer resistance in the circuit. A magnetic field was applied and increased in steps by means of a superconducting niobium solenoid. As the transition temperature was approached the null condition was destroyed due to the change of the magnetic permeability of the sample. To reestablish the null condition M and R were changed and, since ΔM is proportional to the change in the permeability $\Delta\mu$ and, since we start with the superconducting phase ($\mu = 0$), $\Delta M \propto \mu$. A typical plot of μ as a function of the applied field H is shown in Fig. 2. In order to determine the critical field from this plot, we extrapolated the steep linear portion to the normal state permeability μ_n and took the value of H at the intersection as the critical field H_c.

This choice of H_c can be somewhat justified by considering the case of an ellipsoidal sample. The permeability of the superconducting ellipsoidal sample remains zero until $H = (1-n)H_c$ where n is the demagnetizing coefficient of the specimen. At this value of H the field begins to penetrate into the sample and μ starts to rise linearly. The penetration is complete when the sample is entirely normal and μ no longer changes with the field. The situation is demonstrated in Fig. 3.

Since our cylindrical samples are not very different from ellipsoids, we justify our way of choosing H by its analogy to the case of the ellipsoidal sample. Some further justification of this method of critical field determination is given by Mapother and co-workers.[25]

A. <u>The Coil System</u>

The blank and the sample carrying secondary coils, the primary coil,

and the superconducting niobium magnet solenoid were assembled together and will be referred to as the coil system. The description of each component will now be given.

The six indium specimens, five isotopically enriched and one naturally occurring, were put into glass protective containers and placed inside the bakelite sample holders. The secondary coils previously referred to as S were made by winding 1,000 turns of #40 copper wire around the sample holders.

Six of these sample holders were arranged in a circle on a bakelite support that also carried the blank secondary B. By means of a switching device the desired sample containing secondary could be picked and opposed to the blank. This way, during a run at some constant T, we could measure the permeability change of one isotope after another for each increment of the applied field.

The support with the sample holders was anchored inside an assembly of concentric bakelite tubes. The first tube carried the primary coil, denoted as P above, which was made by winding #28 copper wire 12 turns per inch. The remaining bakelite tubes were used for the winding of the niobium solenoid magnet. The magnet consisted of five layers. Each of the first four layers contained 44 turns per inch of 0.005" niobium wire wound along a groove. The outermost layer, the fifth, had two end coils made by winding 176 turns per inch of 0.005" niobium wire in order to insure a high degree of homogeneity. The homogeneity inside a 1" sphere at the center of the solenoid was better than 0.02 per cent. The assembled coil system is shown in Fig. 4.

The magnetic field produced by the superconducting magnet was calculated from the geometry of the coils and the current. The changes in

dimensions on cooling were measured and taken into account in the calculation. A diagram of the circuit used for supplying the solenoid current is given in Fig. 5.

B. Temperature Control and Measurement

The coil system was supported in a cryostat shown schematically in Fig. 6. Above the λ point the temperature of the He bath was regulated by controlling the pumping speed (hence, pressure) above the bath. A very simple pressure regulator[26] performed beautifully in this respect.

Below the λ point, since the thermal conductivity of liquid He is very high and the vapor pressure becomes small, the temperature can be regulated more effectively by means of an electronic regulator. We employed an electronic regulator which has been described by Sommers.[27]

The temperatures were determined from the He vapor pressure measurements by using the 1958 He^4 Temperature Scale.[28] For points above the λ point a heater mounted below the coil system was used to stir the bath and the manometer readings were corrected for the hydrostatic head of liquid He above the samples. Because of the high thermal conductivity of helium II no such correction is necessary below the λ point. Since the hydrostatic head correction amounts to ten to twenty millidegrees near the λ point, its straight forward application might have introduced some inaccuracy in the temperatures within the region just above the λ point. A discussion of the hydrostatic head problem is given by Hoare and Zimmerman.[29]

C. Sample Preparation

400 mg lots of isotopically enriched indium samples were obtained from Oak Ridge National Laboratories. The exact composition of these samples along with that of the natural indium are given in Table I.

Table I. Composition of In Samples

Nominal Composition	Actual Composition
In^{115}	99.5% In^{115}, 0.5% In^{113}
Natural In	95.7% In^{115}, 4.3% In^{113}
25% In^{113}	74.8% In^{115}, 25.2% In^{113}
50% In^{113}	49.76% In^{115}, 50.24% In^{113}
75% In^{113}	24.8% In^{115}, 75.2% In^{113}
In^{113}	3.7% In^{115}, 96.3% In^{113}

The In^{113} and In^{115} samples were provided in bead form, and others as powder. The powdered specimens were heated in small graphite crucibles under 10^{-5} mm Hg and converted into bead form. About 5% of the sample was lost in this process.

The bead form specimen was placed inside a glass tube one end of which had been pulled to a capillary of 0.058" inner diameter as shown in Fig. 7. The specimen was heated to slightly above its melting point in an electric oven at a pressure of 10^{-5} mm of Hg. The inside of the capillary was coated with Octoil-S diffusion pump oil, but shaking was still required to cause the indium to flow inside the capillary. After the casting was completed, the capillary was sealed and cut away by a torch.

An undesirable property of indium is that it sticks to glass while solidifying. This strains the samples causing erratic behavior in the transition curves. Even the oil coating could not prevent the indium from sticking to the glass. To avoid this problem we etched the glass away with concentrated hydrofluoric acid. A 0.05" layer of glass was etched

away in about an hour. Concentrated hydrofluoric acid attacks indium extremely slowly and therefore we did not face the danger of dissolving any of our precious isotopes. The free indium rods were then put into protective glass cases and annealed for 24 hours at about 100°C in order to remove any strains.

3. Results and Discussion

A. Critical Field Values

We have tabulated the critical field values for the six indium specimens in Table II. The precision of our values is within 0.15%; the scatter is mostly due to the random errors made in reading the critical fields from the transition curves. A representative collection of the transition curves is given in Figs. 8 through 13. Since our samples were submerged directly in the He bath, fluctuations in the bath temperature made it very difficult to take permeability measurements in the steep portions of the transition curves at temperatures above the λ-point. Thus we often encountered a situation in which the sample was completely superconducting at one point, and at the next one, corresponding to an increase of only 0.2 Oe, it was entirely normal. Below the λ-point this problem did not exist, but the broadening of the transition curves still made it impossible to determine the critical fields with a precision better than 0.15%.

Although Finnemore[30] claimed better precision in his measurements on natural indium, his points have nearly the same scatter as ours.

With the exception of the points slightly above the λ-temperature there is no reason to believe that any error was made in the temperature determinations outside of what is due to the intrinsic inaccuracy of the 1958 He^4 Temperature Scale. For the points just above the λ-point, as we have said previously, the hydrostatic head correction amounts to a few tens of millidegrees and, even though the bath was stirred by a heater that induced boiling of the liquid below the samples, the accuracy of this correction is questionable.

Table II. Critical Fields of Indium Samples

T	Critical Fields (Oe)					
	In^{115}	Natural In	25% In^{113}	50% In^{113}	75% In^{113}	In^{113}
3.385	3.04	3.35	3.65	4.85	6.13	7.16
3.376	4.67	4.97	5.20	6.54	7.68	8.53
3.262	21.73	22.09	22.41	23.36	24.53	25.50
3.204	29.98	30.36	30.73	31.65	33.15	33.92
3.182	33.5	33.6	34.4	35.3	36.5	37.2
3.042	53.4	53.48	53.91	54.94	56.05	56.95
2.963	64.6	64.9	65.0	66.2	67.3	68.3
2.824	82.9	83.3	83.5	84.4	85.3	86.5
2.745	93.3	93.9	94.0	94.9	96.2	97.0
2.608	110.8	111.2	111.3	112.4	113.6	114.4
2.507	123.0	123.6	123.9	124.5	125.8	126.5
2.406	135.9	136.2	136.3	137.4	138.4	139.0
2.290	149.2	149.3	149.5	150.4	151.2	152.2
2.156	163.3	163.9	164.2	164.9	165.7	166.5
2.070	172.6	172.7	173.1	173.9	174.6	175.7
1.885	190.9	191.1	191.5	192.4	192.8	193.7
1.742	204.1	204.2	204.4	205.3	205.9	206.8
1.591	216.8	217.3	217.5	218.3	219.1	219.7
1.430	229.5	229.8	229.9	230.6	231.4	231.9
1.283	240.0	240.1	240.5	241.2	241.6	242.6
1.219	244.0	244.5	244.1	245.5	246.1	246.5
1.125	249.9	249.9	250.2	251.3	251.4	232.6

B. Isotope Effect

The transition temperatures for the different isotopes were determined by extrapolating the critical field curves to H=0 (see Fig. 14). These are given together with the average isotopic masses in Table III. If the isotope effect is representable by the expression

$$M^{\alpha} T_c = \text{constant},$$

a plot of log M versus log T_c should give a straight line with a slope equal to $-\alpha$. Such a plot is shown in Fig. 15. Within the scatter, the points lie on a straight line with

$$\alpha = +0.50 \pm 0.03.$$

We have thus established that although indium has an abnormal heat capacity behavior, with regard to the isotope effect it behaves like the other soft superconductors.

In the introduction we have said that the isotope effect with $\alpha = +0.50$ is predicted by the BCS theory. Now we would like to point out the arbitrary nature of this prediction. The derivation of the ground state energy of a superconductor by the BCS theory gives

$$W(0) = -\frac{2N(0)(\hbar\omega_c)^2}{\exp[2N(0)/V]-1} \qquad (1)$$

where N(0) is the density of single electron states of one spin at the Fermi Surface, V is the matrix element for the interaction which leads to a transition of a pair of electrons from the state $(\vec{k}\uparrow, -\vec{k}\downarrow)$ to $(\vec{k}\uparrow, -\vec{k}\uparrow)$, and ω_c is a cutoff frequency equal to $k\Theta_D/h$, where Θ_D is the Debye temperature. Since the W(0) is proportional to Θ_D^2, which in turn is inversely proportional to the isotopic mass, we have

Table III. Transition Temperatures of Indium Samples

Isotope	Isotopic Mass	Transition Temperature
In^{115}	114.94	3.406°K
Natural In	114.82	3.408
25% In^{113}	114.44	3.410
50% In^{113}	113.93	3.4175
75% In^{113}	113.44	3.4263
In^{113}	113.01	3.433

$$W(0) \propto M^{-1}.$$

On the other hand,

$$W(0) = \frac{H_o^{\,2} V}{8\Pi}$$

therefore,

$$H_o \propto M^{-1/2}.$$

For a group of isotopes the theory predicts

$$H_o \propto T_c,$$

so that

$$T_c \propto M^{-1/2}.$$

In deriving Eq. (1), the matrix element for the interaction between two electrons is assumed to be

$$V_{kk'} = V \text{ (constant) when } |\epsilon_k| \leq \hbar\,\omega_c$$

$$V_{kk'} = 0 \text{ elsewhere}$$

where ϵ_k is the single electron energy measured from the Fermi Surface. This assumption (which also results in a single energy gap) is quite arbitrary. It is especially unrealistic in that it cuts off the Coulomb repulsion between the two electrons at $\hbar\,\omega_c$. Swihart[31,32] as well as Morel and Anderson[33] have removed this unrealistic cutoff by considering the Coulombic repulsion beyond the range $|\epsilon_k| = \hbar\,\omega_c$ and predicted α to about 20% less than the BCS value. It seems paradoxical that the unrealistic BCS assumption should yield an isotope effect prediction which is in closer agreement with the experimentally observed values for the soft supercondutors. Very recently J. W. Garland[34] reported a new explanation of the isotope effect based on the BCS formalism but including a distinction between s and d electrons. His caluclated values of α are shown in Table IV and are in excellent agreement with experiment. For In Garland predicted $\alpha \approx 0.47$, in excellent agreement with our result.[35]

G. Similarity Principle

The critical field values for In^{113} and In^{115} are plotted in Fig. 16. We have not plotted the critical field curves for the intermediate isotopes because the resolution is not visible on such a scale. However, they lie nicely between the curves for In^{113} and In^{115}.

Since the critical field curves have nearly parabolic shapes with $H_c = H_o(1 - \frac{T^2}{T_c^{\,2}})$, a plot of H_c versus $(\frac{T}{T_c})^2$ is best for extrapolating H_c to 0°K and thus determining the critical field at absolute zero (H_o). In Fig. 17 we show such a plot for natural indium in the range $T < 1.5$°K. Since our points do not extend below 1°K, a reliable extrapolation to absolute zero is not possible. In order to obtain the correct H_o, we made use of Finnemore's[30] data on natural indium which extend to 0.3°K. His

Table IV. Comparison of α Values Calculated by Garland[a] with Experimental Values

Material	Experimental Value for α	Calculated Value
Zn	0.45 ± 0.05	0.40 ± 0.03
Cd	0.50 ± 0.10	0.36 ± 0.04
Sn	0.47 ± 0.02	0.44 ± 0.02
Hg	0.50 ± 0.03	0.47 ± 0.01
Pb	0.48 ± 0.01	0.47 ± 0.01
Te	0.50 ± 0.10	0.45 ± 0.02
Ru	0.00 ± 0.05	0.00 ± 0.20
Os	0.10 ± 0.10	0.10 ± 0.20
Mo	0.37 ± 0.07	0.35 ± 0.07
Nb_3Sn	0.08 ± 0.02	0.20 ± 0.12
Mo_3Ir	0.33 ± 0.03	0.33 ± 0.08

[a] Ref. 34

points, which are systematically 0.17% lower than ours, are also indicated in Fig. 17. For the value of H_o for natural indium we took Finnemore's value and lowered it by 0.17%, thus taking into account the systematically lower values for our H_c's. We could not find the reason for this discrepancy between Finnemore's and our critical field values for natural indium. (In calculating the fields produced by the solenoid, we took into account the thermal contraction of the bakelite coil formers, which was found to be 0.45% between room temperature and liquid helium temperatures.) The lowest-temperature measurements on the isotopically-enriched samples

were consistent with $H_0/H_0' = T_c/T_c'$. To test the similarity principle at high temperatures, we plotted

$$D = h - (1-t^2)$$

as a function of t^2. Now, if the critical field curves did not have similar shapes, this plot would have reflected the deviations from similarity in an amplified fashion. As Fig. 18 shows, the deviations from the parabolic shape are, within the precision of the measurements, the same for all the isotopes.

As mentioned in Part II, there is a connection between the similarity principle and the lattice heat capacity. Chester[8] pointed out that if the similarity principle is obeyed, one can write the critical field H_c as

$$H_c = M^{-\alpha}\,\phi(M^{\alpha}T) \tag{2}$$

where M is the average isotopic mass, T is the temperature and ϕ is a universal function of its argument $M^{\alpha}T$. The difference between the normal and the superconducting state Gibbs Free Energies is related to the critical field by the well known formula

$$G_n - G_s = \frac{H_c^{\,2}V}{8\Pi} \tag{3}$$

where V is the molar volume. If one substitutes Eq. (3) in Eq. (2), one obtains

$$G_n - G_s \sim M^{-2\alpha}\chi(M^{\alpha}T) \tag{4}$$

where the symbol ~ is used to indicate the functional dependence on M and T. Since $C = -T\,\frac{\partial^2 G}{\partial T^2}$, $C_n - C_s$ will have the following functional dependence on M and T:

$$C_n - C_s \sim M^{-\alpha}\ \psi\,(M^{\alpha}T) \tag{5}$$

Any term in C_n that has a different dependence on M and T than that of the right-hand-side of Eq. (5) has to be cancelled by an equivalent term in C_s. Now it is usually assumed that C_n is the sum of two terms; the electronic term γT and the lattice term $C_{\ell n}$. It is furthermore assumed that γT is independent of mass and therefore has the correct dependence on M and T. The lattice term, however, is proportional to $M^{3/2}T^3$ at sufficiently low temperatures[8] and does not have the required form (unless $\alpha = 3/4$). Hence, Chester concludes $C_{\ell n}$ must be cancelled by an identical term in C_s if Eq. (2), that is to say the similarity principle, is valid.

The argument of Marcus and Maxwell[7] that relates the similarity principle to the lattice heat capacities is expressed in the language of the two-fluid model, which was first proposed by Gorter and Casimir.[36] In this model

$$G_n = U_0 - \frac{1}{2}\gamma T^2 + G_\ell(T), \tag{6}$$

and

$$G_s = U_0 - \beta\omega - \frac{1}{2}\gamma T^2 K(\omega) + G_\ell(T). \tag{7}$$

The quantity ω $(0 \leqslant \omega \leqslant 1)$ can be interpreted in several ways, the simplest (and crudest) of which is that it is the fraction of the electrons that have condensed into a single low-energy state and therefore have zero entropy. U_0 is that part of the zero-point energy of the entire system that remains unchanged in the condensation and the term $\beta\omega$ represents the condensation energy. $G_\ell(T)$ is the lattice free energy (here assumed the same in the two states, i.e. independent of ω), $-\frac{1}{2}\gamma T^2$ is the normal-state conduction-electron free energy and $K(\omega)$ is the factor by which it is modified as the condensation proceeds. Apart from questions of interpretation, there are no restrictive assumptions in Eqs. (6) and (7) other than that of equal lattice free energies, as long as the function $K(\omega)$ is

unspecified. The equilibrium value of ω, ω_e, is determined by the condition that $G_s(\omega_e)$ is a minimum, and with the use of Eq. (3), the expression for the reduced critical field becomes

$$h^2 = \omega_e + \frac{1-K(\omega_e)}{K'(0)} t^2. \tag{8}$$

Marcus and Maxwell argued that $K(\omega)$ should not be expected to be an explicit function of M, so ω_e is a function only of t and Eq. (8) gives the similarity principle, in agreement with the measurements[11] on Sn. However, this result would not have been obtained if different expressions for the lattice free energies of the two states had been used, and the observed similarity principle for Sn suggests that the lattice heat capacities are the same for the two states, in agreement with measurements of C_n and C_s for that metal.[6]

If the lattice heat capacities are not assumed equal in the two states, G_ℓ becomes a function of T and ω and Eqs. (6) and (7) must be replaced by

$$G_n = U_0 - \frac{1}{2}\gamma T^2 + G_\ell\,(T,0), \tag{9}$$

and

$$G_s = U_0 - \beta\omega - \frac{1}{2}\gamma T^2 K(\omega) + G_\ell(T,\omega). \tag{10}$$

The equilibrium value of ω is determined by the condition that G_s is a minimum, which is

$$K'(\omega_e) = -\frac{2\beta}{\gamma T^2} + \frac{2}{\gamma T^2}\,\frac{\partial G_\ell(T,\omega_e)}{\partial \omega_e} \tag{11}$$

Relating the critical field to the free energy difference, one obtains

$$\frac{H_c^2 V}{8\Pi} = \beta\omega_e - \frac{1}{2}\gamma T^2[1-K(\omega_e)] + F_\ell(T,0) - F_\ell(T,\omega_e). \tag{12}$$

At $T = 0°K$, $H_c = H_0$, $\omega_e = 1$, and $F_\ell(T,0) = F_\ell(T,\omega_e) = 0$, therefore,

$$\beta = \frac{H_0^2 V}{8\Pi} \quad . \tag{13}$$

Solving Eq. (11) for γ, substituting it in Eq. (12), and making use of Eq. (13), we obtain

$$h^2 = \omega_e + \frac{1-K(\omega_e)}{K'(\omega_e)} - \frac{1-K(\omega_e)}{\beta K'(\omega_e)} \frac{\partial F_\ell(T,\omega_e)}{\partial \omega_e} + \frac{1}{\beta} [F_\ell(T,0)-F_\ell(T,\omega_e)]$$

or

$$h^2 = \omega_e + \frac{1-K(\omega_e)}{K'(\omega_e)} + \Delta$$

where

$$\Delta = - \frac{1-K(\omega_e)}{\beta K'(\omega_e)} \frac{\partial F_\ell}{\partial \omega_e} + \frac{1}{\beta} [F_\ell(T,0) - F_\ell(T,\omega_e)] \quad . \tag{14}$$

The mass dependence of h and the deviation from the similarity principle is contained in Δ.

For indium, the combination of calorimetric and elastic constants data strongly suggests that the lattice heat capacities are different,[6] but, within the precision of the present measurements, the similarity principle is obeyed. The question of whether or not these experimental results are inconsistent with the preceding theoretical arguments requires a quantitative calculation, which neither Chester nor Marcus and Maxwell considered. Furthermore, it requires some kind of an assumption about the way in which any difference between the lattice heat capacities of the two states depends on M, e.g. the dependence of $G_\ell(T, \omega_e)$ on M in the two-fluid model terminology. There is no theoretical guide for such an assumption and therefore any comparison is to a certain extent arbitrary, but as a rough approximation, we take the model described by the following equations.

$$C_n = C_{en} + C_{\ell n}, \; C_s = C_{es} + C_{\ell s} \tag{15}$$

$$\Delta S_e\,(T_c) = \Delta S_\ell(T_c) = 0 \tag{16}$$

$$\Delta C_e = \gamma T - \frac{3\gamma T^3}{T_c^{\,2}} \tag{17}$$

$$\Delta C_\ell = AT^3\left(1 - \frac{4}{3}\,\frac{T}{T_c}\right) \tag{18}$$

$$T_c \propto M^{-1/2} \tag{19}$$

$$A \propto M^{3/2} \tag{20}$$

Here the subscripts e and ℓ refer respectively to the electronic and lattice quantities, S is the entropy, γT is the electronic heat capacity of the normal state, and ΔC stands for $C_n - C_s$, etc. Equation (15) expresses the usual assumption of independent lattice and electron contributions to thermodynamic properties, and Eq. (16) was assumed in order to enable us to treat the electronic and the lattice terms without mixing. Since $\Delta S_e(T_c) + S_\ell(T_c) = 0$, the treatment without mixing is impossible unless we assume each term to be zero. Equation (17) is a commonly employed approximation, equivalent to a parabolic critical field curve. Equation (18) approximates the experimental data on In, for which, at low temperatures, C_{es} and $C_{\ell n}$ are both proportional to T^3 but with different proportionality constants, and for which the difference between C_{es} and $C_{\ell n}$ decreases near 0.5°K. Integrating Eqs. (17) and (18) gives

$$\Delta G_e(T) = \Delta G_{e0} - \frac{\gamma T^2}{2} + \frac{\gamma T^4}{4T_c^{\,2}} \tag{21}$$

$$\Delta G_\ell(T) = \Delta G_{\ell 0} - \frac{A}{12}\,T^4 + \frac{A}{15\,T_c}\,T^5 \tag{22}$$

where the subscript 0 denotes quantities at 0°K. Using the condition $\Delta F_e(T_c) = \Delta F_\ell(T_c) = 0$ [this condition follows directly from Eq. (16)], we obtain

$$\Delta G_{e0} = \frac{\gamma T_c^2}{4} \tag{23}$$

$$\Delta G_{\ell 0} = \frac{A T_c^4}{60} \quad . \tag{24}$$

Substitution of Eqs. (23) and (24) in Eqs. (21) and (22), yields

$$\Delta G_e(T) = \frac{\gamma T_c^2}{4} (1-t^2)^2 \tag{25}$$

$$\Delta G_\ell(T) = \frac{A T_c^4}{60} (1-5t^4 + 4t^5) \tag{26}$$

where $t = T/T_c$. ΔG and H^2 are sums of separate lattice and electronic terms,

$$\Delta G = \Delta G_e + \Delta G_\ell \ , \ H_c^2 = H_{ec}^2 + H_{\ell c}^2 \ . \tag{27}$$

Since $\Delta G = \frac{H_c^2 V}{8}$, by using Eqs. (25) and (26), we get

$$\frac{V H_{ec}^2}{8\pi} = \frac{\gamma T_c^2}{4} (1-t^2)^2 \tag{28}$$

and

$$\frac{V H_{\ell c}^2}{8\pi} = \frac{A T_c^4}{60} (1-5t^4 + 4t^5) \quad . \tag{29}$$

Denoting $\frac{8\pi}{V} \frac{\gamma T_c^2}{4}$ by H_{e0}^2 and $\frac{8\pi}{V} \frac{A T_c^4}{60}$ by $H_{\ell 0}^2$, Eqs. (28) and (29) can be rewritten as

$$H_{ec}^2 = H_{e0}^2 (1-t^2) \tag{30}$$

$$H_{\ell c}^2 = H_{\ell 0}^2 (1-5t^4 + 4t^5). \tag{31}$$

An important consequence of Eqs. (28) and (29) is that

$$H_{e0} \propto M^{-1} \tag{32}$$

$$H_{\ell 0} \propto M^{-1/2} \tag{33}$$

because we have assumed that $T_c \propto M^{-1/2}$ and $A \propto M^{3/2}$.

In order to estimate the deviation from the similarity principle, we shall now derive an expression for $\frac{\delta H_c}{H_c}$ where δH_c is the change in the critical field corresponding to a change δM in the isotopic mass. Combining Eqs. (30) and (31) with Eq. (27), we obtain

$$H_c^2 = H_{e0}^2 (1-t^2)^2 + H_{\ell 0}(1-5t^4 + 4t^5)$$

Differentiating this with respect to M, we arrive at

$$2H_c \left(\frac{\partial H_c}{\partial M}\right)_T dM = \frac{dH_{e0}^2}{dM}(1-t^2)^2 + \frac{dH_{\ell 0}^2}{dM}(1-5t^4 + 4t^5) \quad dM \tag{34}$$

From Eqs. (32) and (33), we get

$$\frac{dH_{e0}^2}{dM} = (-1)\frac{H_{e0}^2}{M}$$

$$\frac{dH_{\ell 0}^2}{dM} = (-\frac{1}{2})\frac{H_{\ell 0}^2}{M}$$

Substituting these in Eq. (34) and noting that $\delta H_c = \left(\frac{\delta H_c}{\delta M}\right)_T dM$, one obtains

$$2H_c \delta H_c = -\frac{H_{e0}^2}{M}(1-t^2)^2 - \frac{H_{\ell 0}^2}{2M}(1-5t^4 + 4t^5) \quad dM$$

or

$$\frac{\delta H_c}{H_c} = \Delta' \frac{dM}{2M} \tag{35}$$

where

$$\Delta' = \frac{-H_{e0}^2(1-t^2) - \frac{H\ell_0^2}{2}(1-5t^4 + 4t^5)}{H_{e0}^2(1-t^2)^2 + H_{\ell 0}^2(1-5t^4 + 4t^5)}$$

If we now take $\gamma = 1.69$ millijoules degree^{-2} mole^{-1}, and

$A = 0.22$ millijoules degree^{-4} mole^{-1}, in accordance with the measurements on In and remember that

$$H_{e0}^2 = \frac{8\Pi}{V} \frac{\gamma T_c^2}{4}$$

and

$$H_{\ell 0}^2 = \frac{8\Pi}{V} \frac{A T_c^4}{60},$$

we obtain the following expression for Δ':

$$\Delta' = - \frac{4.90(1-t^2)^2 + 0.246\ (1-5t^4 + 4t^5)}{4.90(1-t^2)^2 + 0.492\ (1-5t^4 + 4t^5)} \tag{36}$$

In Table V some representative values for Δ' are given together with the corresponding $\delta H_c/H_c$ values which were obtained by using Eq. (35) for the In^{113} and In^{115} samples. The $\delta H_c/H_c$ are less than those predicted by the similarity principle (0.0088 for $t \approx 1$) by such small amounts that they could not be observed experimentally.

Table V

t	Δ'	$\frac{\delta H_c}{H_c}$
0	-0.944	0.0083
0.1	-0.943	0.0083
0.2	-0.939	0.0082
0.3	-0.933	0.0082
0.4	-0.925	0.0081
0.6	-0.903	0.0079
0.8	-0.872	0.0077
1.0	-	-

In conclusion, the precision to which the similarity principle has been tested for In is not inconsistent with the small difference between C_{es} and $C_{\ell n}$ that may exist at low temperatures.[6] It could perhaps be used to rule out appreciably larger discrepancies such as the one originally reported for In by Bryant and Keesom[3] but even this would require an assumption about the way in which $C_{es} - C_{\ell n}$ depends on M. The only other test of the similarity principle (for Sn) is of comparable precision and the effect of sample shape, strains, and impurities on H_c makes it unlikely that this can be significantly improved. Since other metals appear to show discrepancies between C_{es} and $C_{\ell n}$ that are at least no larger than that for In, it appears the similarity principle is not a useful criterion for the equality of C_{es} and $C_{\ell n}$ as proposed by Chester and Marcus and Maxwell.

Part I

REFERENCES

1. B. S. Chandrasekhar and J. A. Rayne, Phys. Rev. Letters 6, 3 (1961).
2. G. A. Alers and D. L. Waldorf, Phys. Rev. Letters 6, 677 (1961).
3. C. A. Bryant and P. H. Keesom, Phys. Rev. Letters 4, 460 (1960).
4. H. R. O'Neal, Ph.D. Thesis, University of California (1963).
5. H. R. O'Neal, N. M. Senozan and N. E. Phillips, Proceedings of the Eighth International Conference on Low Temperature Physics (London, 1962), Butterworths, Washington (1963).
6. H. R. O'Neal and N. E. Phillips, Phys. Rev. in press.
7. P. M. Marcus and E. Maxwell, Phys. Rev. 91, 1035 (1953).
8. G. V. Chester, Phys. Rev 104, 883 (1956).
9. E. Maxwell, Phys. Rev 91, 1035 (1953).
10. C. A. Reynolds, B. Serin, W. H. Wright and L. B. Nesbitt, Phys. Rev 78, 487 (1950).
11. J. M. Lock, A. B. Pippard and D. Shoenberg, Proc. Cambridge Phil Soc. 47, 811 (1951).
12. E. Maxwell, Phys. Rev 86, 235 (1952).
13. B. Serin, C. A. Reynolds, and C. Lohman, Phys. Rev. 86, 162 (1952).
14. E. Maxwell, Nat. Bur. Standards, Circular #519 (1952).
15. M. Olsen, Nature 168, 245 (1951).
16. R. R. Hake, D. E. Mapother and D. L. Decker, Phys. Rev. 112, 1522 (1958).
17. D. L. Decker, D. E. Mapother and R. W. Shaw, Phys. Rev. 112, 1888 (1958).
18. H. Frohlich, Phys. Rev. 79, 845 (1950).
19. J. Bardeen, L. N. Cooper and J. R. Schrieffer, Phys. Rev. 108, 1175 (1957).
20. T. H. Geballe, B. T. Matthias, E. Corenzwit and G. W. Hull, Phys. Rev. Letters 6, 275 (1961).

21. T. H. Geballe and B. T. Matthias, I.B.M. J. Res. Develop. 6, 256 (1962).

22. B. T. Matthias, T. H. Geballe, E. Corenzwitt and G. W. Hull, Phys. Rev. 129, 1025 (1963).

23. G. E. Devlin and E. Corenzwitt, Phys. Rev. 120, 1964 (1960).

24. R. A. Erickson, L. D. Roberts and J. W. T. Dabbs, Rev. Sci. Instr., 25, 1178 (1954).

25. J. F. Cochran, D. E. Mopother and R. E. Mould, Phys. Rev. 103, 1657 (1956).

26. E. J. Walker, Rev. Sci. Instr. 30, 834 (1959).

27. H. S. Sommers, Jr., Rev. Sci. Instr. 25, 793 (1954).

28. F. G. Brickwedde, H. van Dijk, M. Durieux and J. K. Logan, J. Res. Natl. Bur. Standards 64A, 1 (1960).

29. F. E. Hoare and J. E. Zimmerman, Rev. Sci. Instr. 39, 184 (1959).

30. D. Finnemore, Ph.D. Thesis, University of Illinois (1961).

31. J. C. Swihart, Phys. Rev. 116, 45 (1959).

32. J. C. Swihart, I.B.M. J. Res. Develop. 6, 14 (1962).

33. P. Morel and P. W. Anderson, Phys. Rev. 125, 1263 (1962).

34. J. W. Garland, Jr., Phys. Rev. Letters 11, 114 (1963).

35. J. W. Garland, Jr., private communication.

36. C. J. Gorter and H. B. G. Casimir, Z. Phys. 35, 963 (1934).

Part I

FIGURE CAPTIONS

Fig. 1 Schematic diagram of the inductance bridge.

Fig. 2 A typical transition curve.

Fig. 3 The transition curve for an ellipsoid with demagnetization factor n.

Fig. 4 The coil system.

Fig. 5 Circuit for providing and measuring the current in the superconducting solenoid.

Fig. 6 Schematic drawing of the cryostat.

Fig. 7 Glass tube for casting indium samples.

Fig. 8 Transition curve for In^{115}, 25% In^{113}, and 75% In^{113} at 3.3851°K.

Fig. 9 Transition curve for Natural In, 50% In^{113}, and In^{115} at 3.3851°K.

Fig. 10 Transition curve for In^{115}, 50% In^{113}, and In^{115} at 2.8239°K.

Fig. 11 Transition curve for Natural In, 50% In^{113}, and In^{115} at 2.8239°K.

Fig. 12 Transition curve for In^{115}, 50% In^{113}, and In^{115} at 1.4300°K.

Fig. 13 Transition curve for Natural In, 50% In^{113}, and In^{115} at 1.4300°K.

Fig. 14 Extrapolation of the critical field curves to $H_c = 0$.

Fig. 15 Effect of isotopic mass on transition temperature.

Fig. 16 Critical Field vs. Temperature for In^{113} and In^{115}.

Fig. 17 Critical field vs. the square of the reduced temperature for natural indium.

Fig. 18 Deviations of the critical fields from parabolas for the indium samples. Deviations from the similarity principle would show up as systematic differences between the different samples.

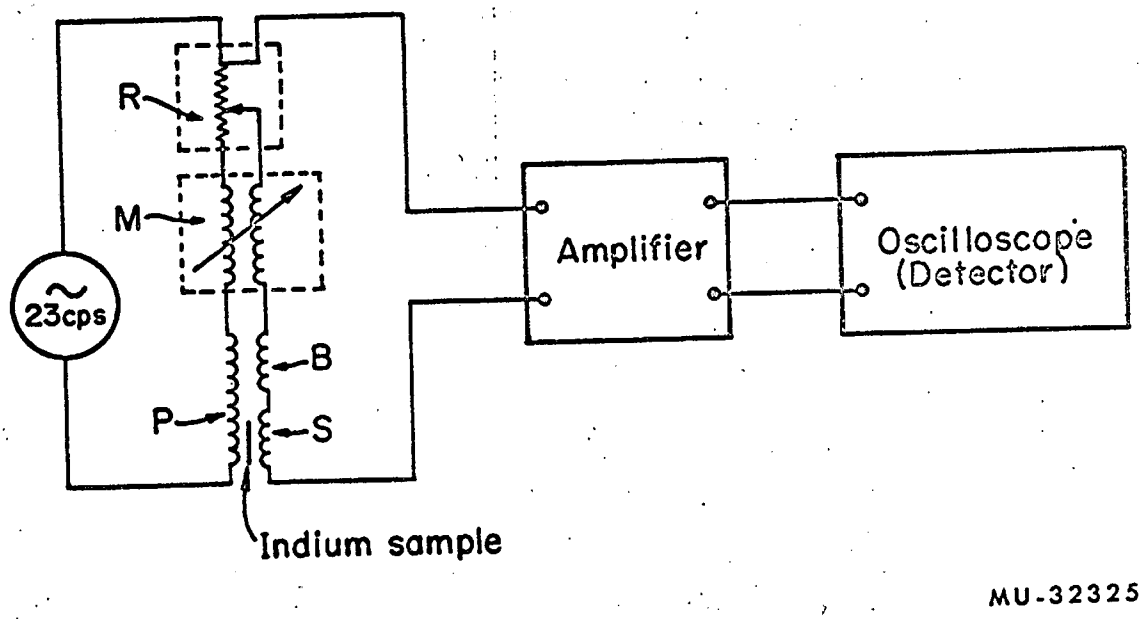
R
M
23cps
B
P
S
Indium sample
Amplifier
Oscilloscope
(Detector)
MU-32325

Figure 1

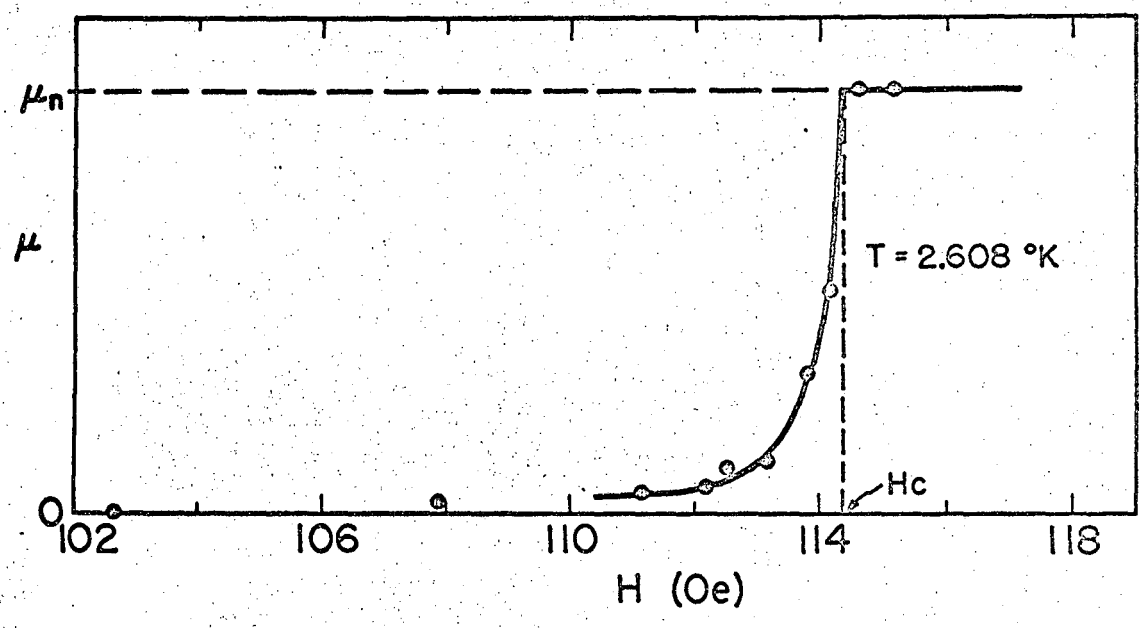

MU-32327

Figure 2

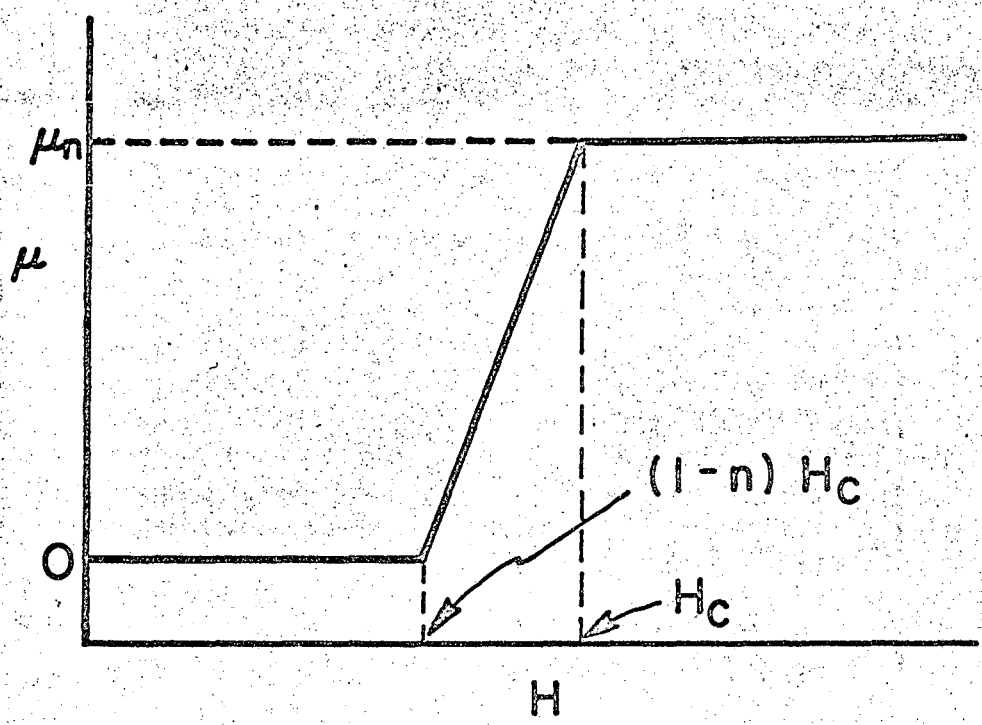

MU-32328

Figure 3

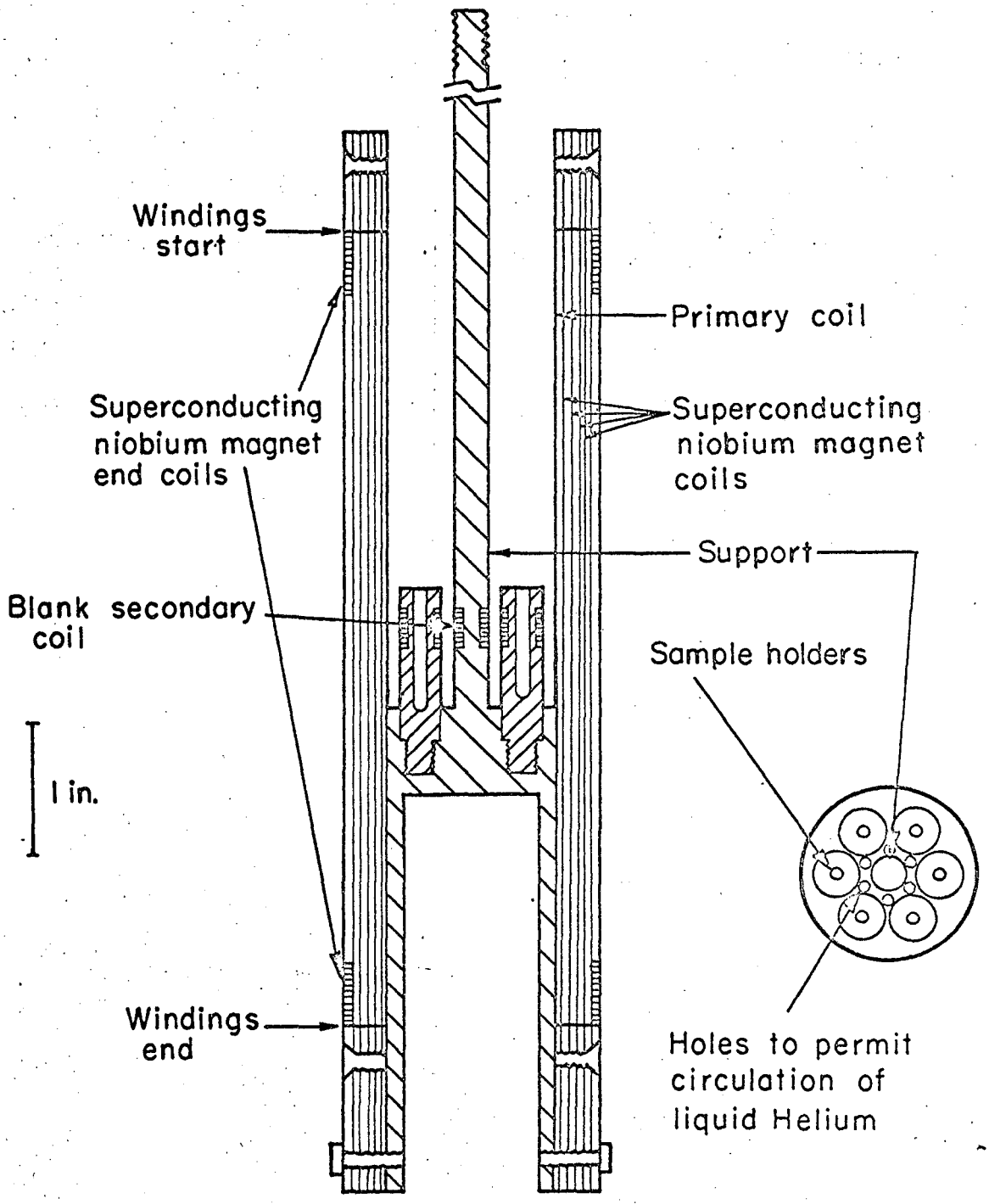

MU-32331

Fig. 4

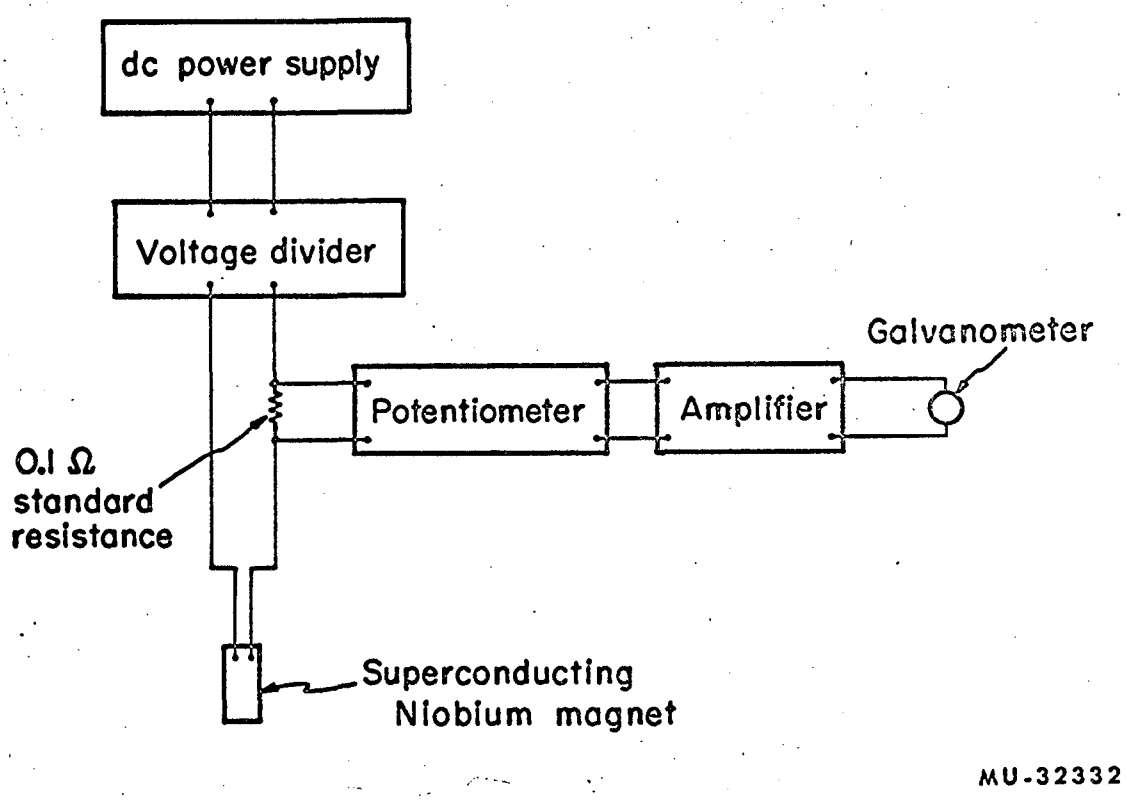
dc power supply
Voltage divider
Galvanometer
Potentiometer
Amplifier
0.1 Ω
standard
resistance
Superconducting
Niobium magnet
MU-32332

Figure 5

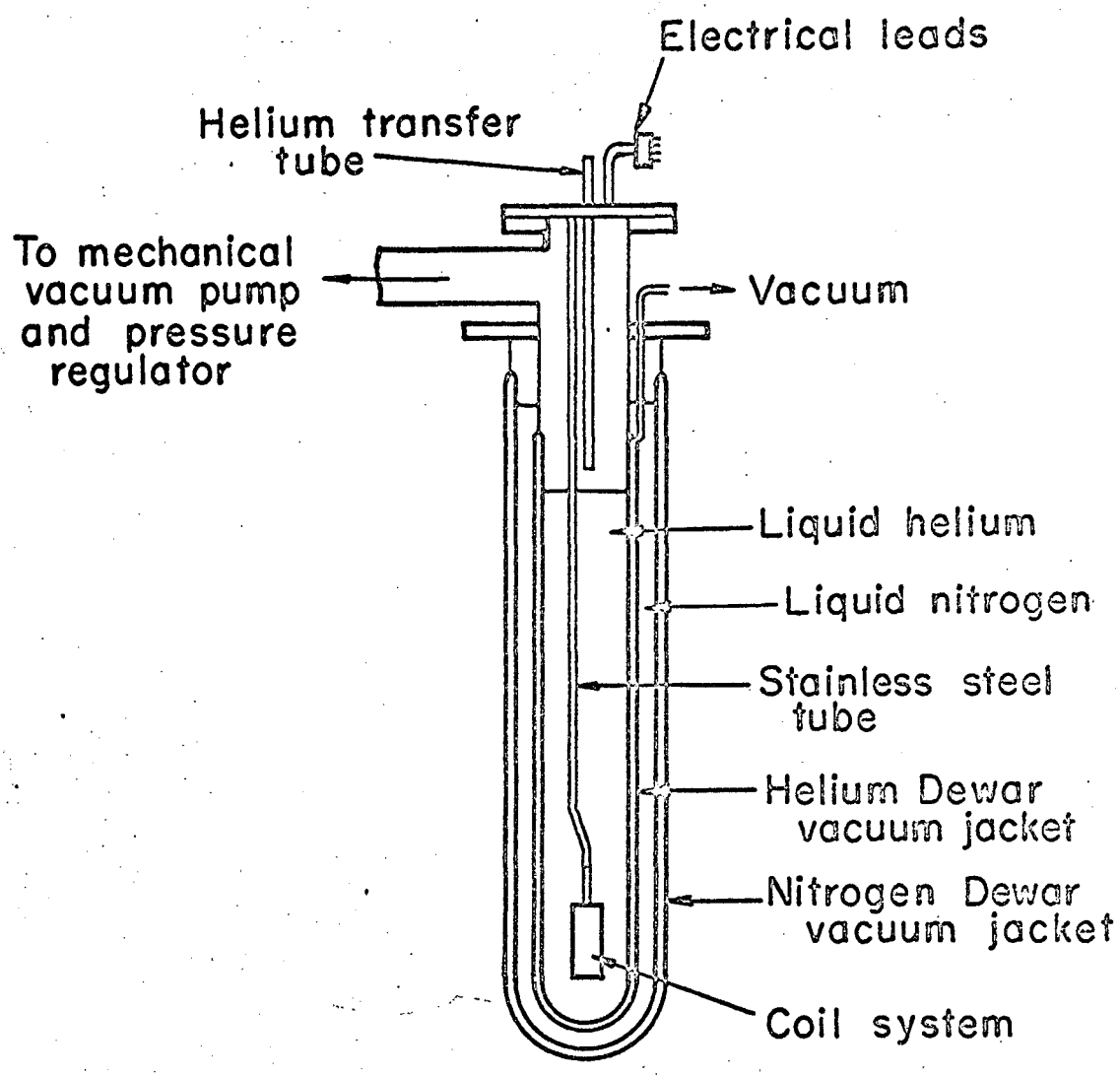

MU-32333

Figure 6

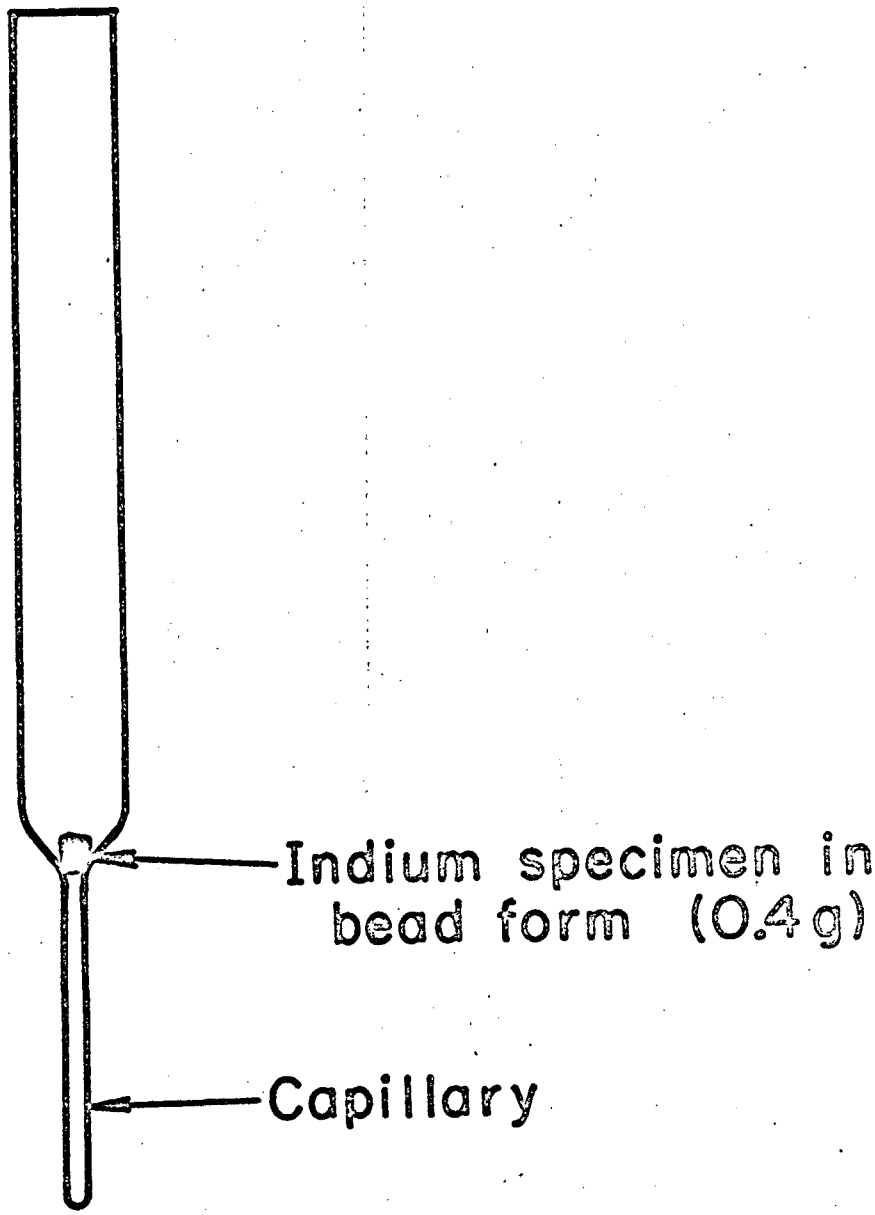

MU-32335

Figure 7

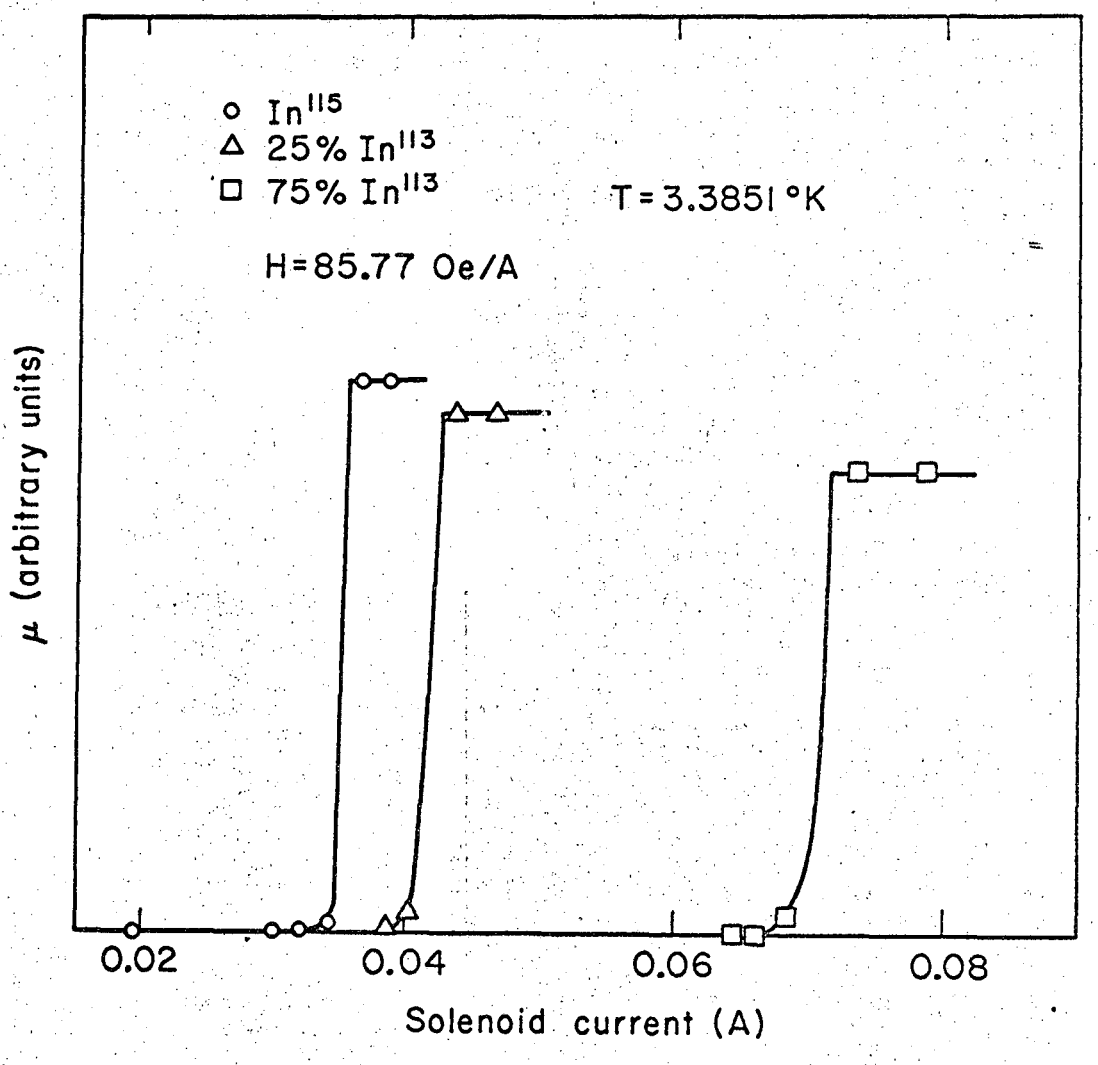

MU-35189

Figure 8

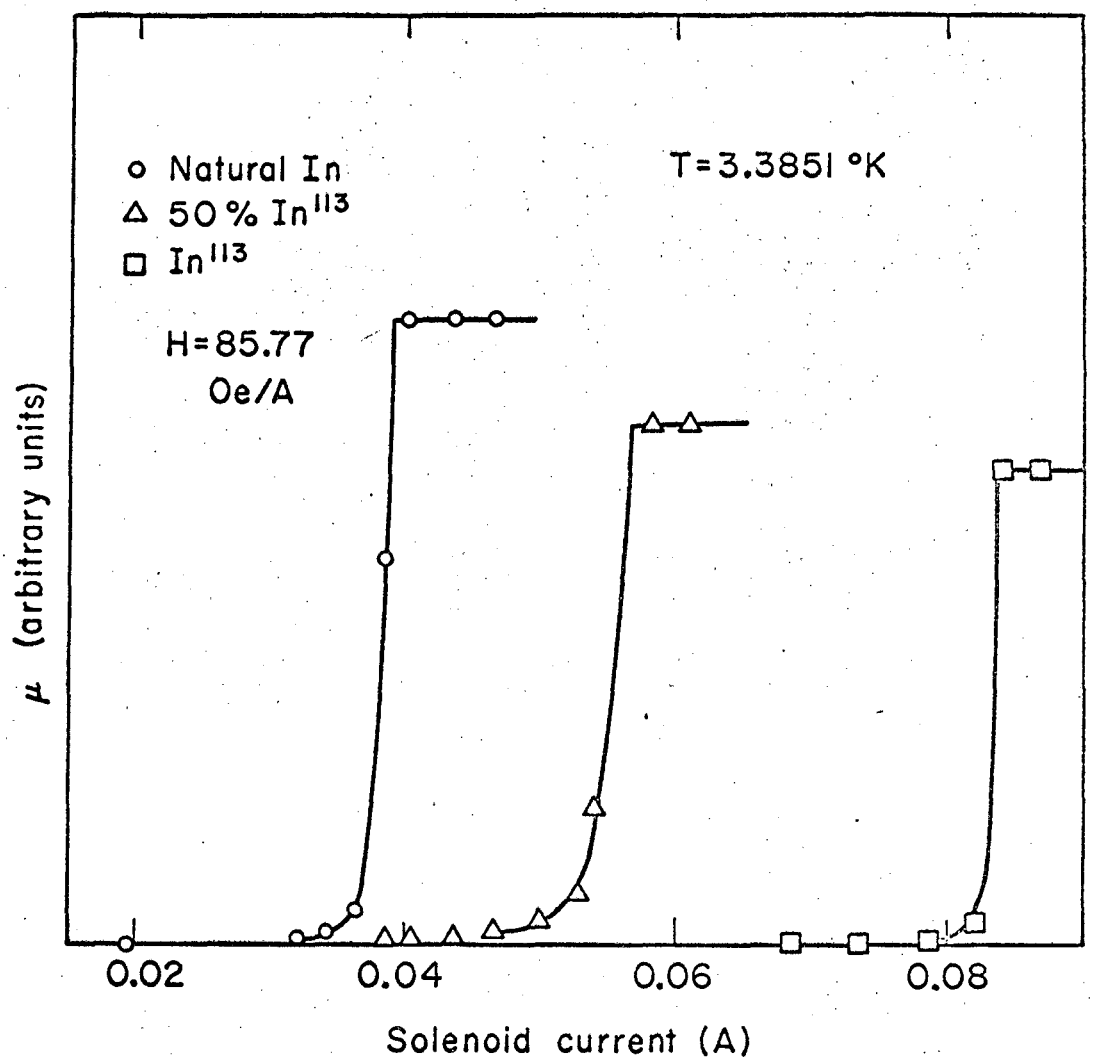

MU-35190

Figure 9

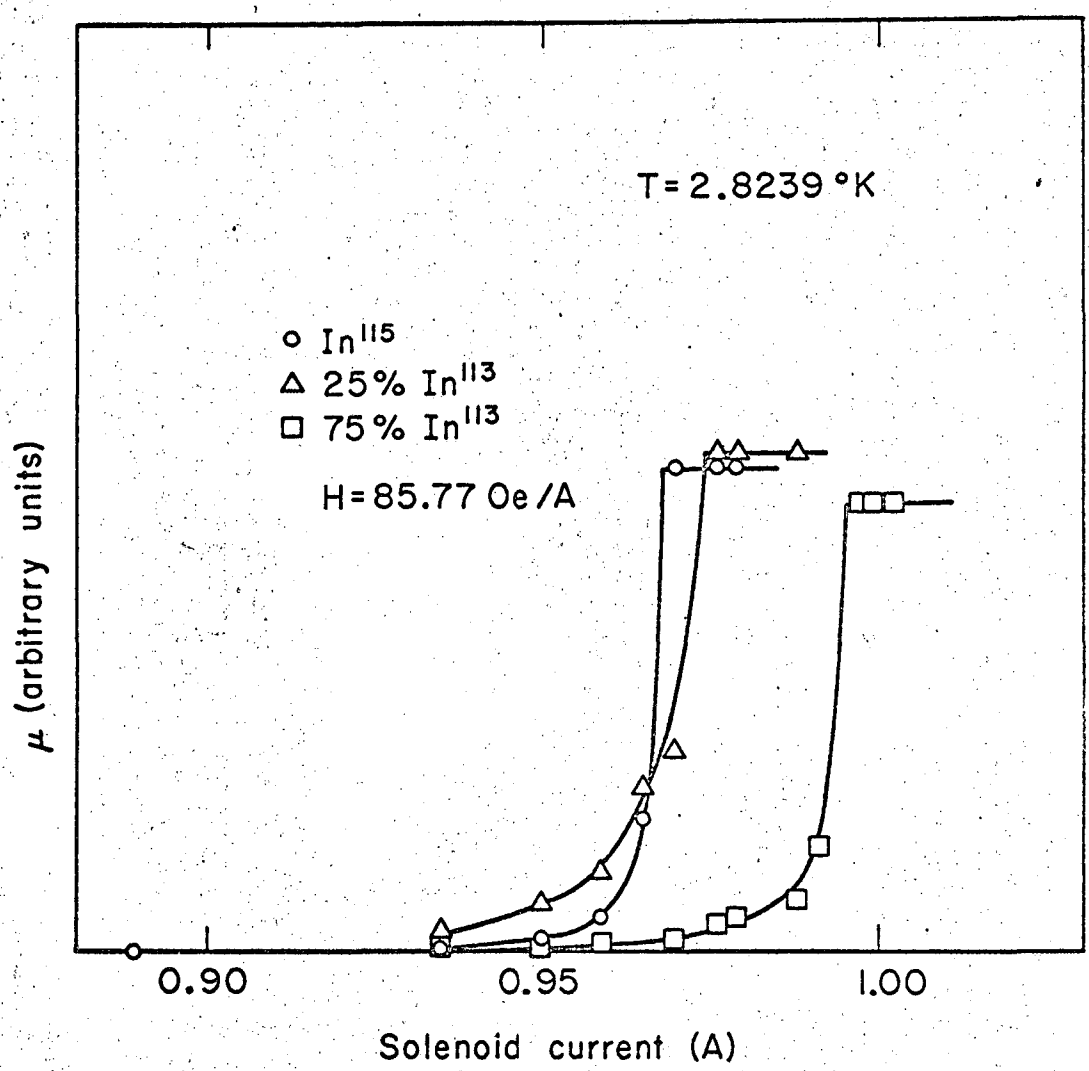

MU-35191

Figure 10

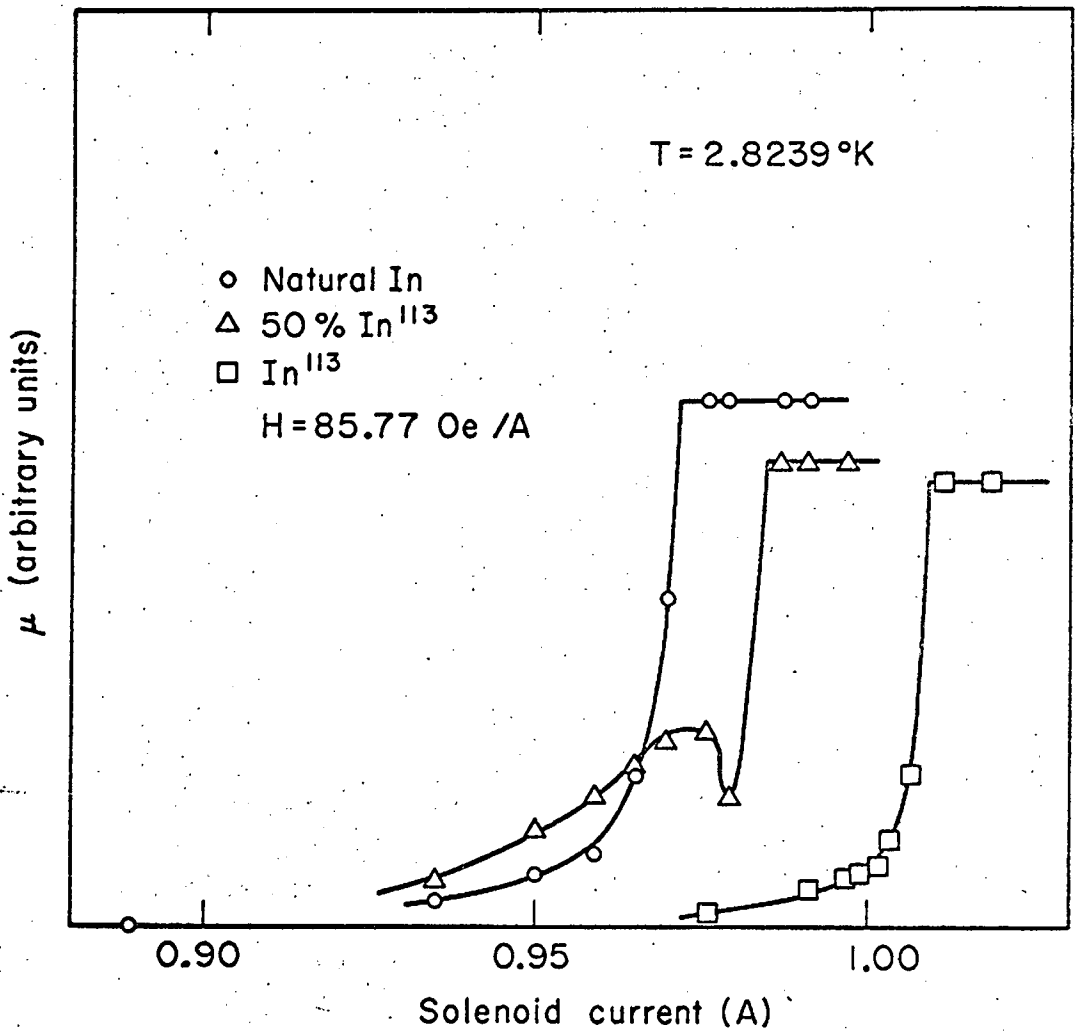

MU-35192

Figure 11

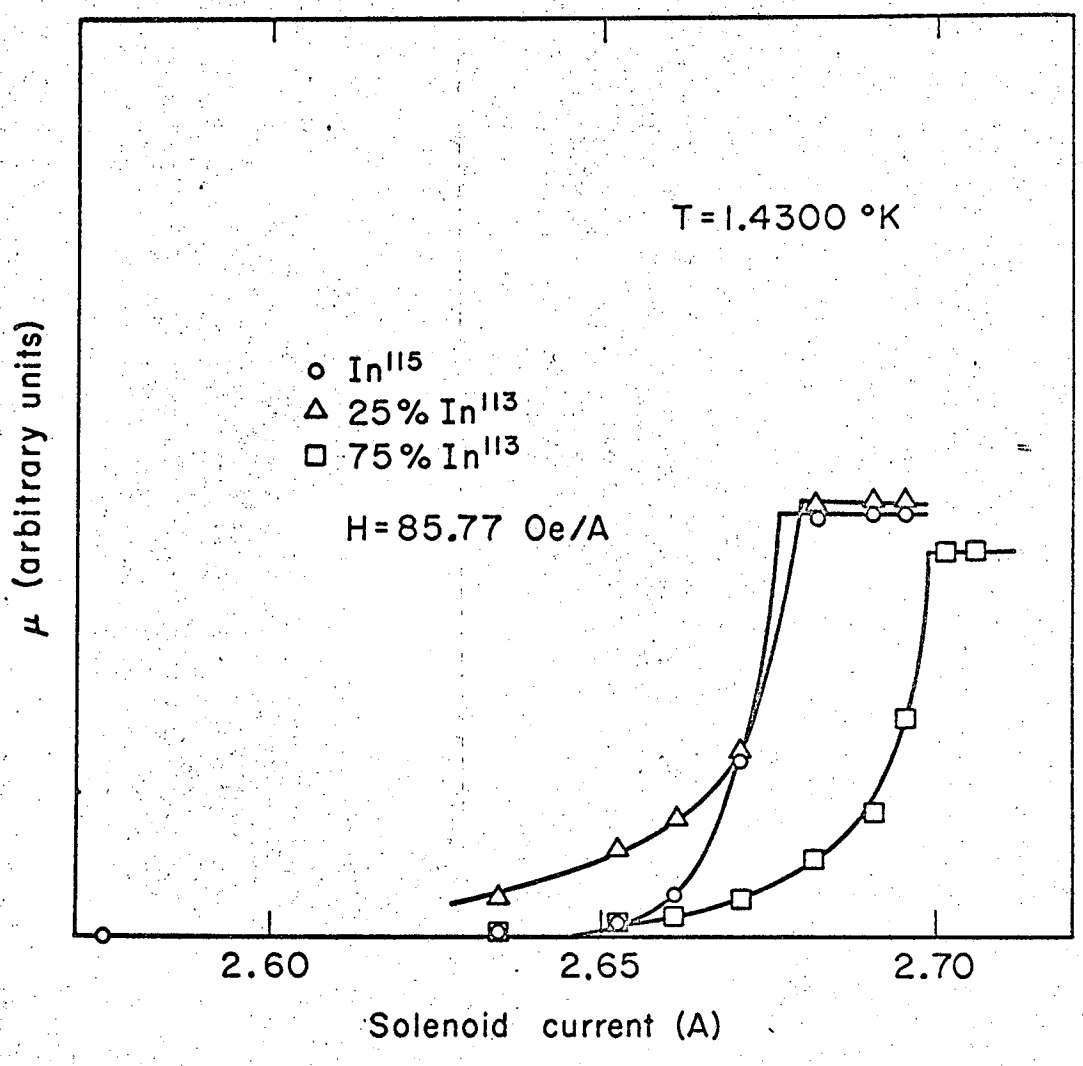

MU-35193

Figure 12

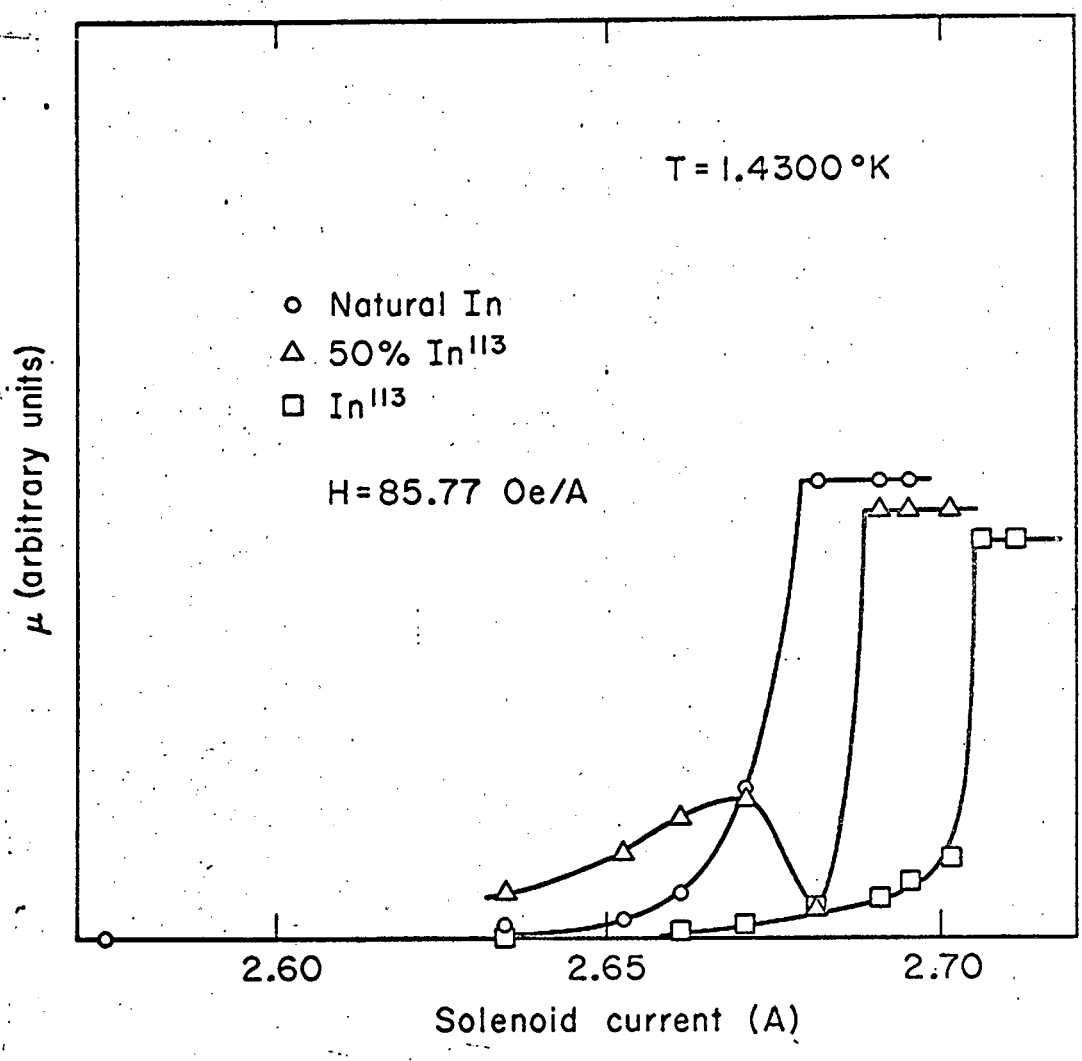

MU-35194

Figure 13

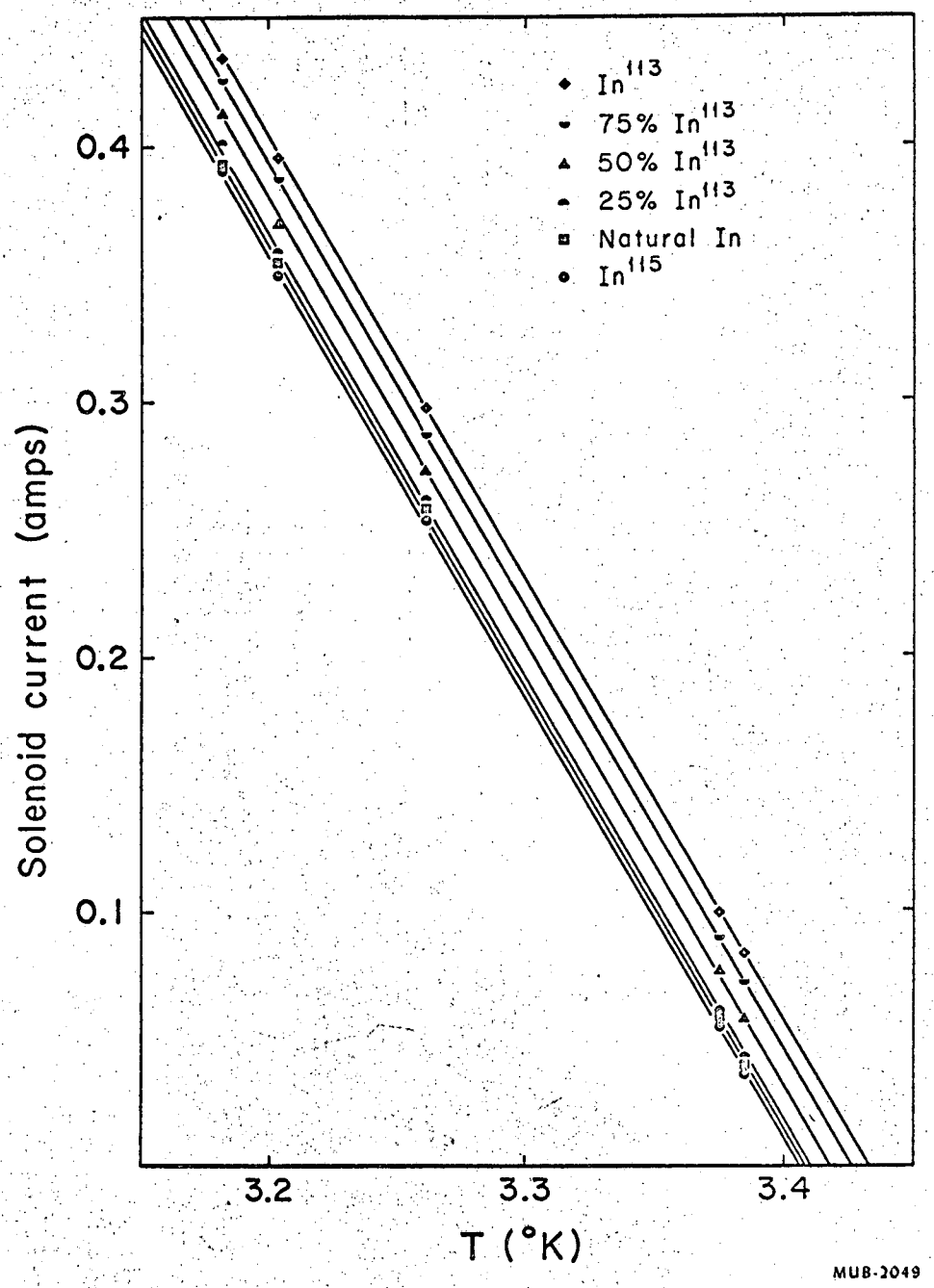
In113
75% In113
50% In113
25% In113
Natural In
In115
0.4
0.3
0.2
0.1
Solenoid current (amps)
3.2
3.3
3.4
T (°K)
MUB-2049

Figure 14

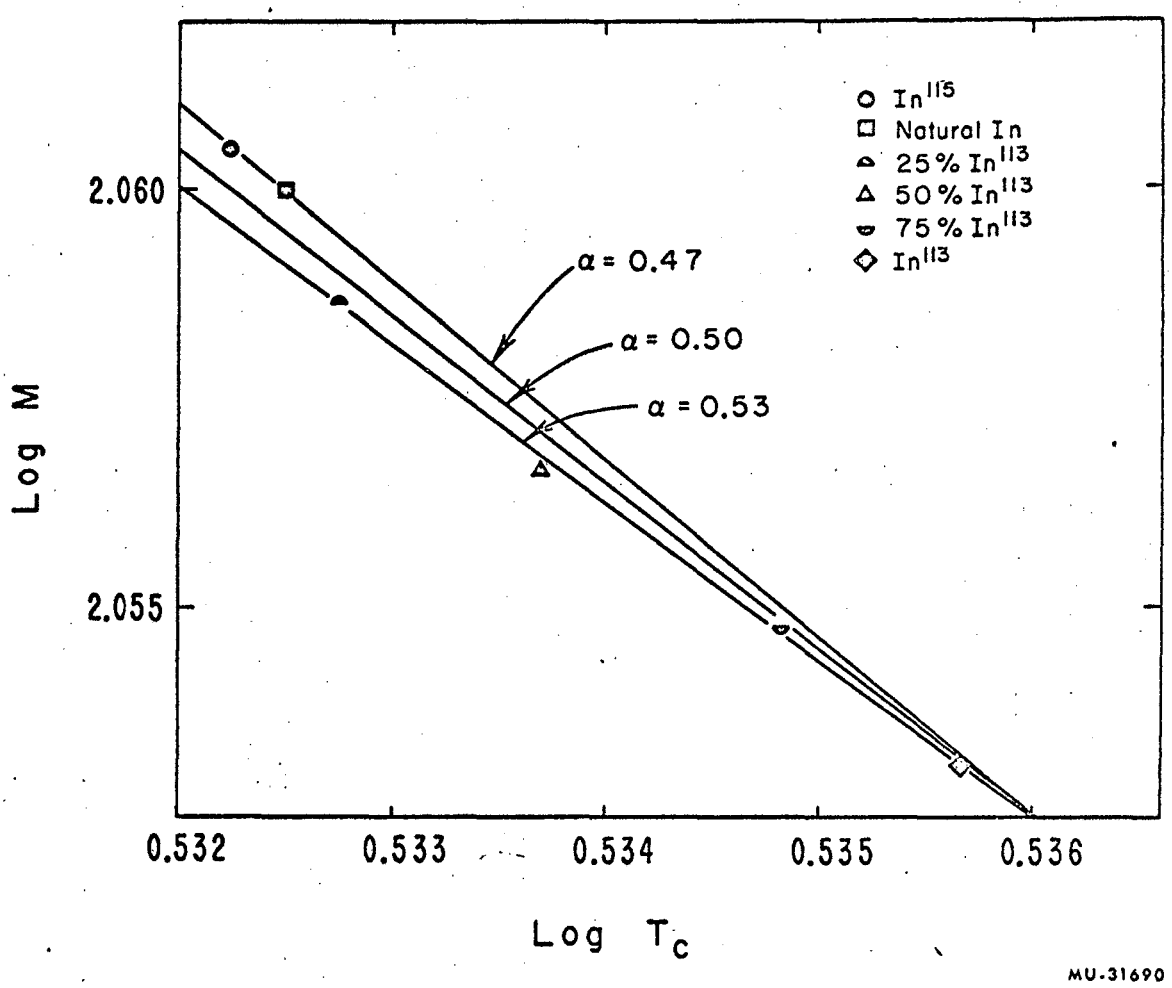
In115
Natural In
25% In113
50% In113
75% In113
In113
α = 0.47
α = 0.50
α = 0.53
2.060
2.055
Log M
0.532
0.533
0.534
0.535
0.536
Log Tc
MU-31690

Figure 15

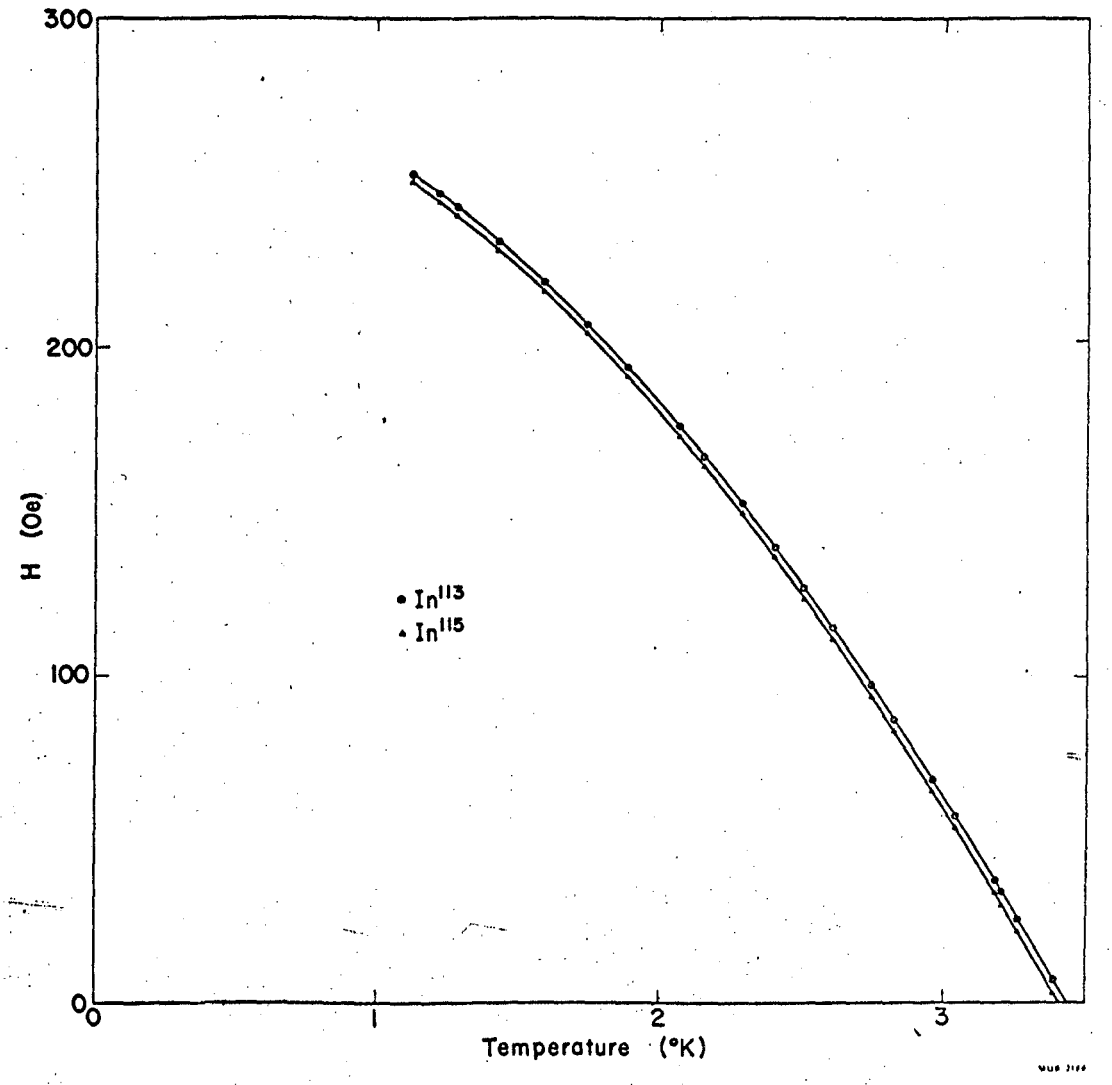

Figure 16

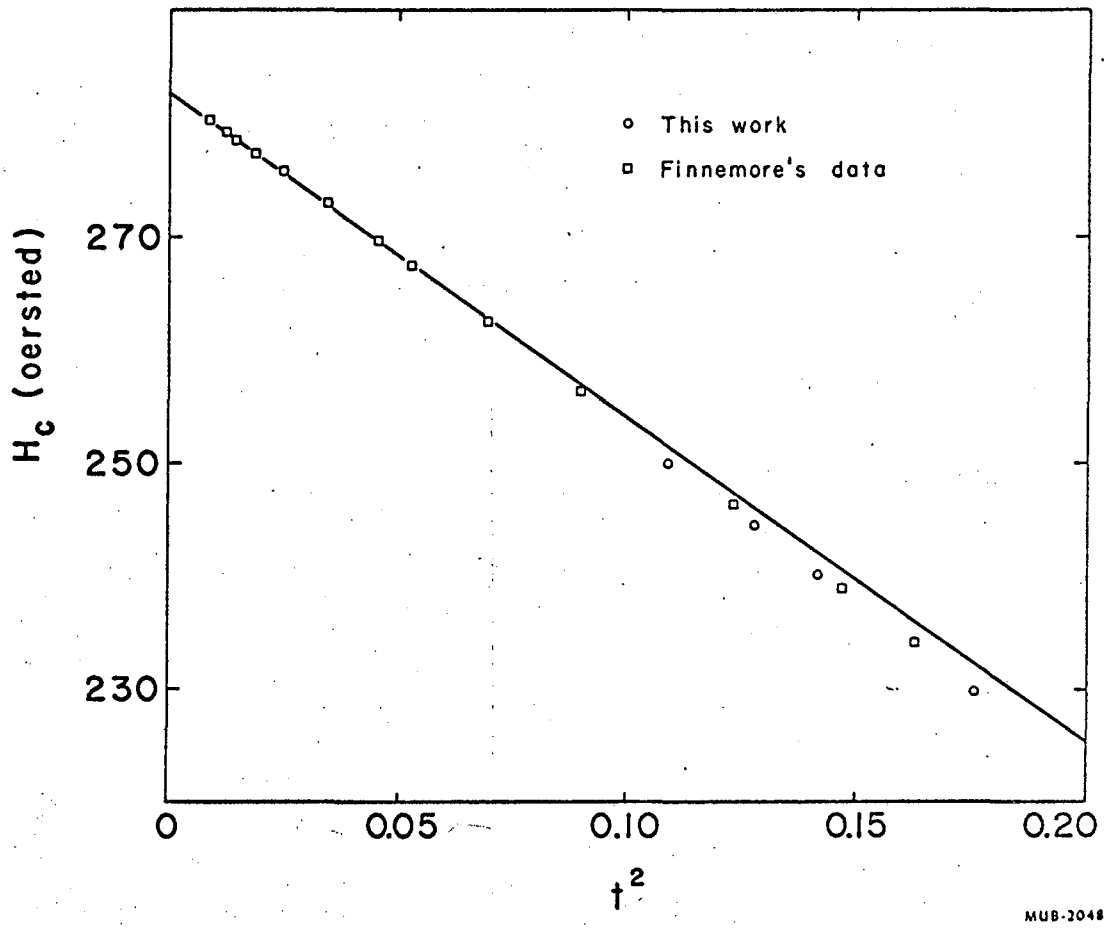
This work
Finnemore's data
270
250
230
H_c (oersted)
0
0.05
0.10
0.15
0.20
t^2
MUB-2048

Figure 17

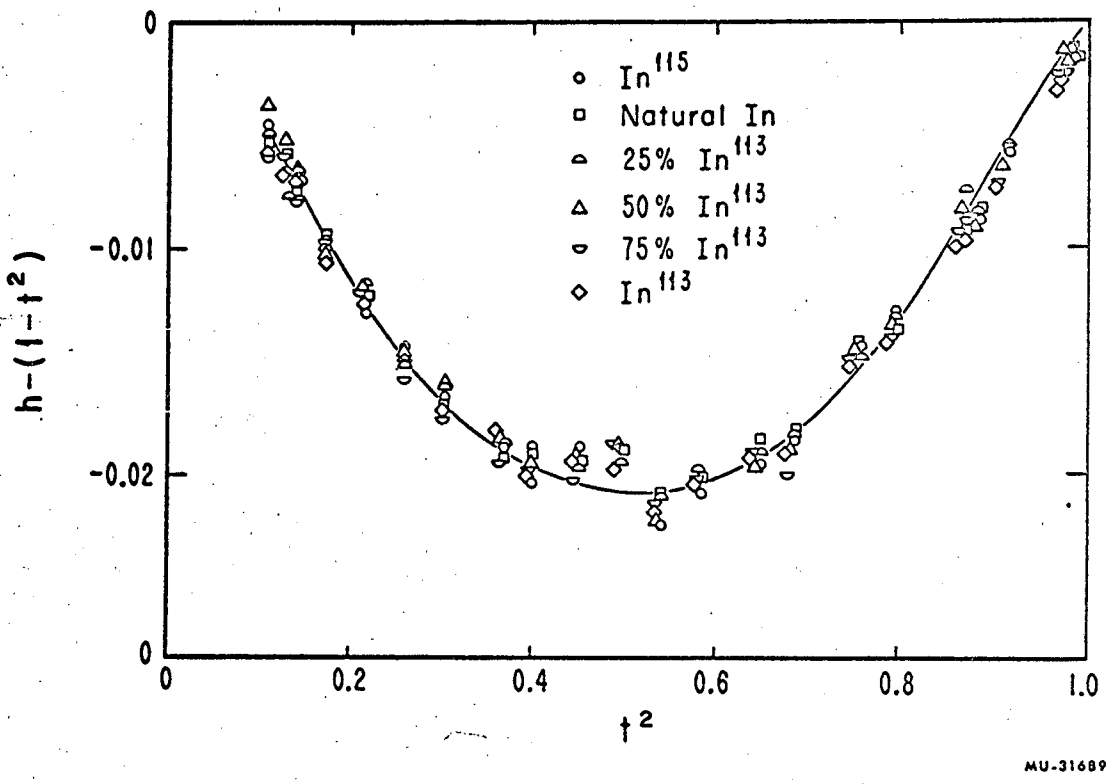
0
-0.01
-0.02
0
0
0.2
0.4
0.6
0.8
1.0
$h-(1-t^2)$
t^2
In^{115}
Natural In
25% In^{113}
50% In^{113}
75% In^{113}
In^{113}
MU-31689

Figure 18

II. LOW TEMPERATURE HEAT CAPACITY OF NIOBIUM

1. Introduction

It is customary to express the low temperature heat capacities of normal and superconducting states of a metal as a sum of electronic and lattice contributions:

$$C_s = C_{es} + C_{\ell s}$$

$$C_n = \gamma T + C_{\ell n}$$

where γT is the normal state electronic heat capacity, C_{es} is the superconducting state electronic heat capacity and $C_{\ell s}$ and $C_{\ell n}$ are the superconducting and normal state lattice heat capacities. As pointed out in Part I of this thesis, the BCS theory predicts, and certain indirect experimental evidence suggests, that in general, $C_{\ell s} = C_{\ell n}$. However, the heat capacity measurements suggest that for indium this is not the case, and more recently theoretical work has been undertaken to provide possible explanations for a difference between $C_{\ell s}$ and $C_{\ell n}$. The situation at present is confused. In order to study the consequences of this discrepancy we undertook the critical field measurements on indium isotopes as described in Part I. Next we wanted to investigate the lattice heat capacities of other metals to see whether the anomaly in indium is unique or whether it is a common property of superconductors.

The determination of the superconducting state electronic and lattice heat capacity is possible only if the electronic term becomes a negligible part of the total heat capacity at low temperatures. Since, according to the BCS theory, the electronic term varies with the reduced temperature T/T_c as $ae^{-b(T_c/T)}$ where a and b are constants, this condition is fulfilled

for metals with high transition temperature and/or small Debye temperatures. In addition to indium, the only superconductors for which it is feasible to investigate and compare the normal and superconducting lattice heat capacities are lead, mercury, tin, thallium, vanadium, tantalum, and niobium. For tin,[1,2] mercury,[3] and lead[3] there appears to be no anomaly, although for lead there are also experiments that suggest that $C_{\ell s} > C_{\ell n}$.[4] For niobium, Hirschfeld et al., whose measurements started from 1.2°K, reported anomalous behavior,[5] but there is some reason to question their conclusions.[3] Furthermore, niobium with its high transition temperature is well suited for studying the lattice heat capacities. In view of the reported anomaly, the absence of any data below 1.2°K, and its suitability, we undertook measurements on niobium extending from 0.25 to 25°K.

Reliable superconducting state measurements on hard superconductors such as niobium are difficult in adiabatic demagnetization cryostats. The magnetizing field leaves frozen in flux in the sample thus causing some normal state material to remain during the superconducting state measurements. So, for this reason, we built a He^3 calorimeter designed to measure heat capacities between 0.25 and 25°K. The description of this calorimeter is given in Section 2. In Section 3 the measurements on the niobium sample are briefly mentioned. The final two sections are devoted to the analysis and discussion of the data.

2. A Calorimeter for Temperatures from 0.25 to 25°K

There are two kinds of calorimeters for work below 1°K. Adiabatic demagnetization calorimeters employ demagnetization of paramagnetic salts and can produce temperatures to well below 0.1°K. In He^3 calorimeters pumped liquid He^3 is the coolant and temperatures as low as 0.25°K can be reached.

The obvious advantage of an adiabatic demagnetization cryostat is that lower temperatures can be obtained. There are, however, cases in which it is mainly the region above 0.25°K that is of interest and particularly here there are serious drawbacks associated with the use of adiabatic demagnetization calorimeters. In this type of apparatus the accuracy of calibration of a thermometer attached to the sample is limited by the warming rate of the salt and the relaxation time characterizing thermal equilibrium between the salt and the sample. At the higher temperatures the salt has a rapidly decreasing heat capacity resulting in a greater drift rate and at the same time the relaxation time usually increases because the heat capacity of the sample increases more rapidly with temperature than the thermal conductivity of the superconducting heat switch employed in this type of apparatus. The magnetic field necessary for magnetizing the paramagnetic salt may in some cases have undesirable effects on the sample under study (e.g. in superconductors it may leave frozen-in flux that affects the measured superconducting state heat capacity). Furthermore, the problem of making and breaking thermal contact in a He^3 calorimeter can be handled in a way that permits the extension of measurements to temperatures well above 1°K. When measurements both above and below 1°K are of interest it is obviously advantageous to make them in the same apparatus. In the remainder of Section 2 an apparatus for

heat capacity measurements between 0.25 and 25°K is described.

A. General Description

Figure 1 shows a schematic drawing of the calorimeter. The heart of the calorimeter is a copper block that can be regulated at any temperature between 0.25° and 25°K. It is supported in an evacuated container surrounded by a liquid He^4 bath. The block can be placed in thermal contact with the surrounding bath through a mechanical heat switch, cooled below 1°K by pumping on liquid He^3 in an attached chamber, or maintained at temperatures above 4°K by supplying heat at a controlled rate. A second mechanical heat switch is used to make thermal contact between the block and the calorimetric sample.

The He^3 chamber and the copper block are made of oxygen free high conductivity (OFHC) copper. The probe of an electronic temperature regulator is attached with varnish to the copper block. The probe consists of a 1000Ω heater made of manganin wire and three Allen Bradley (AB) radio resistor thermometers with resistances of 12Ω, 57Ω, and 170Ω. The functioning of this regulator together with the description of the associated electronic circuits is given by H. S. Sommer Jr.[6] At temperatures between 1° and 10°K, the regulation is very rapid; in fact it is possible to take a set of 40 calibration points in this range in about three hours. At higher temperatures as the heat capacities of the block and sample become larger, the regulation becomes slower. Around 20°K a single calibration point requires as long as one hour. With liquid He^3 in the chamber the operation is unsatisfactory, presumably because liquid He^3 has a high heat capacity and low thermal conductivity. Below 1°K the block temperature is regulated by controlling the speed of pumping on the He^3.

The sample is rigidly mounted with cotton threads inside a brass

cage fastened to the copper block by a set of four screws. A 1200Ω heater of 0.0015" manganin wire is wound and varnished on a small round copper foil and is fastened to the sample. The thermal contact between the copper foil and the sample is provided by Apiezon grease.

The calorimeter space is evacuated by a diffusion pump (Consolidated Vacuum Corporation MCF 60) through a 1/2" stainless steel tube labeled "Calorimeter Evacuating Tube" in Fig. 1. A movable cap acting as a radiation shield is attached to the bottom of this tube. During the evacuation of the calorimeter space the cap is lowered and the end of the tube is kept open, but during the measurements it is pulled up and thus stray radiation is prevented from entering the calorimeter space. The electrical leads are brought inside the calorimeter space at room temperature through Cenco seals and are carried down via two 3/16" stainless steel tubes.

A vapor pressure bulb made of OFHC copper is used in temperature measurements between the λ point (2.2°K) and 4.2°K. Above the λ point helium is a very poor conductor, therefore, the vapor pressure above the bath will not correspond to the temperature of the calorimeter. Furthermore, an accurate temperature correction is impossible because of the difficulty in estimating the effect of the hydrostatic pressure. Hence, in order to determine the temperature correctly above the λ point, the vapor pressure of the helium in the bulb is measured.

The tube going from the vapor pressure bulb to the manometers is vacuum jacketed. Some authors[7] favor this construction; they believe that without the vacuum jacket cold spots may develop causing erroneous pressure readings. On the other hand, certain authors[8,9,10] claim that self-quenching makes the cold spot formation impossible. Furthermore,

they assert that when there is a vacuum jacket the heat leak through the inner tube results in high temperature readings. Evidently the usefulness of a vacuum jacket is debatable.

The superconducting magnet is made from 0.010" niobium-zirconium wire. It produces ~ 1000 Oe per ampere at the center and ~ 500 Oe per ampere at a point 6.5 cm from the center.

Hydrogen exchange gas at 500 micron pressure is used to cool the copper block and sample to 78°K. At that temperature the exchange gas is pumped out and the mechanical heat switches are used to cool to liquid He^4 temperatures. During heat capacity measurements the He^4 bath is usually maintained at 1°K and the block adjusted to a temperature that gives sufficiently small drifts in sample temperature.

After the sample cools to 0.25°K the heat switch is opened carefully. Opening the switch in two steps minimizes the increase in sample temperature; after cooling from room temperature the first breaking of the contact generates an appreciable amount of heat and, in order to re-cool, we close the switch lightly - just enough to make contact. The second breaking of the contact introduces about 50 ergs to the sample. After the sample is isolated the heat capacity points are taken in intervals of T/10 or less. Two typical heating curves for two heat capacity points are shown in Fig. 2. The temperature increment is determined by extrapolating the initial and the final drifts to the middle of the heating period. The heating period is measured by an electronic timer, accurate to 1 millisecond, that is triggered by the same relays that control the heater current. A constant heater current is taken from a regulated power supply and is determined by measuring potentiometrically the voltage drop across a standard resistance in series with the heater.

For the 14 mole copper sample it was possible to take all the specific heat points in a single series of measurements extending from 0.25° to 25°K. Because of the small heat capacity of the niobium sample in the superconducting state it was impossible to take heat capacity points from 0.25° to 25°K in a single run. Instead, the block temperature was adjusted from time to time as the drifts became intolerable.

B. He^3 System

The He^3 system contained 10 ℓ (STP) of He^3, equivalent to about 12 ml of liquid, but only a fraction of this was used in most runs. The He^3 was obtained from the Mound Laboratory. Table I gives its composition.

Figure 3 shows a schematic drawing of the He^3 system. The gaseous helium is stored in the two tanks. Ordinarily one of these tanks contains most of the He^3. At the beginning of the experiment the entire system except the tanks and the space between the exhaust of the main pump and the tanks is evacuated by the auxiliary mechanical pump. When the evacuation is complete valves A and B are closed not to be opened again until the experiment is finished. Since the exhaust of the auxiliary pump opens to air, it is never used while handling He^3.

When the calorimeter is cooled to the lowest temperature attainable by pumping on the He^4 bath, the He^3 is condensed. First valve C is opened and the He^3 inside the exhaust line is allowed into the chamber. Naturally this heats the block and a few minutes must elapse before the temperature returns to its initial value. The main pump (DuoSeal, Model 1405 KBG, with sealed shaft) is then turned on and its exhaust is opened to the He^3 chamber by opening valve D. By opening valves E (or F depending on whichever tank is full) and G we enable the pump to transfer He^3 from the tank to the He^3 chamber. After about 1 ml of liquid is transferred we close

TABLE I

ANALYSIS OF THE He^3 OBTAINED FROM THE MOUND LABORATORY

Element	Abundance
He^3	99.89%
He^4	0.04%
N_2	0.07%
Radioactive impurity	9.67×10^{-8}%

valve E and again wait for the block to cool. Then the whole process is repeated. It takes about fifteen minutes to transfer 8 ml of liquid He^3. When the transfer is finished valves E and F are closed and kept so during the rest of the experiment.

In order to cool the calorimeter below 1.1°K the He^3 chamber is opened to the main pump. The exhaust of this pump is connected to an empty tank. The pumping speed is adjusted by three valves, L, M, and N connected in parallel. L is a Hoke needle valve, M is a 1/2" and N is a 1" Veeco valve. While we could not regulate the block temperature electronically, with some effort regulation was possible by adjusting the pumping speed. With the 1" Veeco valve open, 0.4°K could be reached. In order to go below this the diffusion pump (Consolidated Vacuum Corporation MCF300) was used. The lowest temperature obtained was 0.26°K.

In cooling the calorimeter from 1.1° to 0.3°K with 8 ml of He^3 initially in the chamber, 1.3 ml of He^3 evaporates. Since the heat capacity of He^3 is much larger than that of the block and sample, the heat of this evaporation is taken almost entirely from the He^3 itself. Ordinarily then one fifth of a given amount of He^3 will be consumed in cooling the calorimeter. The heat leak to the block is minute. As a matter of fact, long before the He^3 evaporates it is necessary to transfer He^4. This, however, is not serious because it can be accomplished without an appreciable evaporation of He^3.

C. Mechanical Heat Switches

The heat switches used in this apparatus incorporate several improvements over others that have been used in this laboratory. They are operated by an air cylinder and piston that pushes on a 1/2" X 0.020" stainless steel tube. This stainless steel tube in turn pushes on a rod

that presses on the arms of the switch thus causing the jaws to close. (See Fig. 1.) In order to open the switch the piston is pushed up by applying pressure from the other side. Instead of passing through the calorimeter evacuating tube, the stainless steel tubes that operate the heat switches pass through the He^4 bath and are sealed to the vacuum jacket with metal bellows. This design eliminates heat leak from room temperature to the switch jaws. The only heat leak is to the jaws of the lower switch. This comes only from the temperature of the He^4 bath and is minimized by a thermal shunt of stranded copper between the rod and the He^3 chamber.

An advantage of this design with air cylinders is that the load at the jaws can be calculated from the pressure in the cylinder and can be reproducibly adjusted.

A flexible copper wire was used to thermally attach the jaws of the upper switch to the vapor pressure bulb and the jaws of the lower switch to the block. The thermal resistance between a copper wire clamped in the jaws of a switch and the point of thermal attachment of the jaws was measured. Figure 4 shows the results of these measurements. The data of this figure were obtained with an 8 cm 16 gauge copper wire as the thermal link. The conductivity increases rapidly when the pressure is raised from 10 psi to 20 psi but after that remains fairly constant. This indicates that the conductivity through the switch becomes comparable to that of the 8 cm long copper wire at 20 psi and beyond this pressure it is the wire that limits the conduction.

In 1958 Berman and Mate[11] measured the thermal conductivity between various surfaces at low temperatures. They found that the conductivity varies approximately with the 3/4 power of the load when the dimensions

of microjunctions (where true contact occurs) are large compared to the electron and phonon mean free paths. For copper the microjunctions are of the order of 10^{-2} cm and the mean free paths even at 4°K are not more than 10^{-3} cm. Hence we may assume that the conductivity of our switch would have increased rapidly with the pressure had the 8 cm long wire not been present to limit the conductivity. For the experiments represented in Fig. 4 the jaws of the heat switch were gold plated copper and the wire clamped between them was copper. The observed thermal conductivity at low load is in approximate agreement with that found by Berman and Mate for copper-copper junctions.

In order to give some further idea of the effectiveness of the switches we may cite the following observations; a 14 mole sample of copper cooled from 78°K to 4.2°K in three hours, and from 20°K to 4.2°K in thirty minutes. When this observation was made 50 psi pressure was applied and, as one should bear in mind, the limiting factor was again the copper wire between the sample and the switch. We have also observed that if the switch is pressurized to 60 psi first and then the pressure is released without breaking the contact at the jaws, the conductivity remains unchanged until the pressure drops to about 10 psi.

D. Temperature Measurements

Two germanium resistance thermometers (Minneapolis Honeywell Series II, Probe Type, Special) were used in the measurements. One of these was permanently fixed to the copper block and calibrated as described in the following paragraphs. The second was attached to the sample holder and calibrated against the first by comparing their resistances with the lower mechanical switch closed. Periodic tests of the reproducibility of the two thermometers have been made and no evidence of any instability has

been found.

For the block thermometer calibration the apparatus was arranged as shown in Fig. 5. Three layers of cerium magnesium nitrate crystal, $Ce_2Mg_3(NO_3)_{12}\cdot 24H_2O$, (CMN) were glued together and cut to form hemispheres. These hemispherical pieces were then glued (using General Electric 7031 varnish) to a 0.003" thick copper foil and supported by the lucite holder. The lucite holder as shown in Fig. 5 was tightly mounted to the brass cage which in turn was fastened to the block. The copper foil was soft soldered to a 16 gauge copper wire at a point far enough from the salt to prevent any interference of the solf solder with susceptibility measurements. A Leeds and Northrup platinum resistance thermometer calibrated by the National Bureau of Standards in the range of 10°K - 92°K and a 100Ω Allen Bradley radio resistance thermometer were also attached to the block.

In the 1° to 4°K range the germanium block thermometer was calibrated directly on the 1958 He^4 vapor pressure scale by closing the upper mechanical switch and making simultaneous measurements of vapor pressure and resistance. Above 2.2°K the vapor pressure bulb was used and below 2.2°K the vapor in the He^4 bath was measured. At the same time the Allen Bradley thermometer was calibrated and the mutual inductance of a set of coils surrounding the CMN crystal was measured.

Below 1.1°K the germanium thermometer was calibrated against the magnetic susceptibility of the CMN crystal. The susceptibilities were measured by an a-c bridge method of the type described by Erickson, et al.[12] The Curie Law is well established[13] at the temperatures of interest for this salt and consequently the mutual inductance M of the surrounding coils is a linear function of T^{-1}:

$$M = M_\infty + \frac{A}{T} \qquad (1)$$

M_∞ and A are determined from a plot of M versus T^{-1} between 1° and 4°K. Temperatures below 1°K are then found from the M readings using Eq. (1).

One may wonder whether the method used for the temperature determinations below 1°K can also be applied in the difficult region between 4° and 10°K. In general it can be applied, but for CMN this is not possible. The ground state of Ce^{+++} splits into three doublets by the crystal field - the spacing between the two lowest doublets being 34k (k = Boltzmann's constant).[14] Above 4°K the upper level will begin to be appreciably populated and consequently the Curie Law will no longer be applicable.

Between 10° and 25°K the germanium thermometer and the Allen Bradley thermometer were calibrated against the platinum thermometer.

Temperatures between 4° and 10°K were based on an interpolation of the resistance-temperature (R-T) relation for the Allen-Bradley thermometer. This thermometer was chosen for the interpolation because it is known to fit a simple R-T relation in the 1° to 4° and 15° to 20°K regions.[15] It is therefore plausible that the same relation holds between 4° and 10°K and this assumption has frequently been used. In the present case the best justification for it is based on a consideration of the heat capacity measurements on copper described later in this section. The R-T data for the Allen-Bradley thermometer were fit by an equation of the form

$$\frac{1}{T} = \frac{k_1}{\log R} + k_2 + k_3 \log R + k_4 \log^2 R + k_5 \log^3 R \; . \; . \; . \qquad (2)$$

The fractional difference between the observed temperature T_o at some point and the temperature T_c calculated from Eq. (2) for the same point, $\frac{T_o - T_c}{T_c}$, was plotted as a function of the calculated temperature and this

"difference plot" was used to correct the temperature evaluated from the resistance on the basis of Eq. (2). Equation (2) fit the data to within 1% over the entire range (1.6° to 25°K). In order to make an extreme test of how well Eq. (2) represents the R-T relation we also applied it to the R-T data obtained in the range of 10°K to 25°K and extrapolated to 4°K, and to the R-T data in the range of 1.6°K to 4.2°K and extrapolated to 10°K. The temperatures evaluated on the basis of these two extrapolations differed by about 1% from the correct values. Hence the temperatures calculated on the basis of Eq. (2) should be good to within 1% at the very outside.

We fit the resistance of the block germanium thermometer to various analytical expressions covering three overlapping regions: Between 0.26°K and 1.6°K and also between 1° and 6°K we fit the R-T data to an equation of the form

$$\frac{1}{T} = \frac{k_1}{\log R} + k_2 + k_3 \log R + k_4 \log^2 R + k_5 \log^3 R \quad . \; . \; . \quad (3)$$

Between 4° and 25°K we used another expression of the form

$$\frac{1}{T} = k_0 + k_1 R + k_2 R^2 + k_2 R^3 + k_4 R^4 + k_5 R^5 \ldots\ldots \quad (4)$$

The difference plots were drawn for each region and were used to correct the temperatures calculated from Eqs. (3) and (4). In drawing them, we made sure that in each overlapping region the two plots yielded the same corrected temperature.

The germanium thermometer on the sample was calibrated against the block germanium thermometer. It was possible to fit the R-T data of the former within 2% to two expressions of the form

$$\frac{1}{T} = k_0 + k_1 \log R + k_2 \log^2 R + k_3 \log^3 R + k_4 \log^4 R + k_5 \log^5 R \ldots \quad (5)$$

Again we drew difference plots and used them to correct the calculated temperatures.

Thermometer resistances were determined by measuring the voltage across the thermometer and the thermometer current. The thermometer current was supplied by batteries and was stabilized with high series resistance. It was measured potentiometrically by measuring the voltage drop across a standard resistance in series with the thermometer. The voltage across the thermometer was compared with a known voltage taken from a potentiometer and the difference was amplified and displayed on a recording potentiometer.

Some characteristics of the two germanium thermometers are given in Tables II and III. The resistance becomes power dependent above a certain current, presumably because the power maintains a temperature difference between the germanium element and the capsule. As seen in Table III, the power dependence of the sample thermometer is not too pronounced. It is not troublesome for the block thermometer either above 0.45°K. Below this temperature however, the resistance of this thermometer becomes drastically power dependent and remains so even at the lowest feasible measuring currents. The sensitivity of the thermometers to power level occurs at temperatures for which the thermometers are extremely sensitive. It is possible, particularly for the lower resistance thermometer, to obtain a good temperature sensitivity even at currents for which the power dependence can be ignored. At high temperatures the temperature coefficient becomes small but at these temperatures it is possible to use a large measuring current. Their low noise level, compared with that of some carbon thermometers is important in utilizing this possibility; the noise level in the

Table II. Characteristics of the Block Germanium Thermometer

T °K	R Ω	$\frac{dR}{dT}$ Ω/°K	i μ amp	δR Ω	δT °K corresponding to noise	δT °K corresponding to δR
25	10.4	.52	200	0	$.000^{0}$	0
			300	0	$.000^{0}$	0
20	13.3	.73	200	0	$.000^{0}$	0
			300	0	$.000^{0}$	0
15	18.0	1.4	200	0	$.000^{0}$	0
			300	.005	$.000^{0}$	.003
10	29.6	3.9	100	0	$.000^{0}$	0
			200	.005	$.000^{0}$	.001
			300	.015	$.000^{0}$	.004
6	58.4	13	20	0	$.000^{0}$	0
			50	.002	$.000^{0}$	$.000^{2}$
			100	.05	$.000^{0}$	.004
4	96.3	25	10	0	$.000^{2}$	0
			20	.03	$.000^{1}$	.001
			50	.04	$.000^{0}$	.002
			100	.13	$.000^{0}$	.005
			200	.50	$.000^{0}$	.020
2	220	170	3	0	$.000^{1}$	0
			10	.05	$.000^{0}$	$.000^{3}$
			20	.2	$.000^{0}$	.001
			50	1.3	$.000^{0}$	.008
1	640	1300	1	0	$.000^{1}$	0
			3	.1	$.000^{0}$	$.000^{1}$
			5	1	$.000^{0}$	.001
			10	2	$.000^{0}$	.002
			20	10	$.000^{0}$	.008
.7	1400	5000	1	0	$.000^{1}$	0
			3	.5	$.000^{0}$	$.000^{1}$
			5	1.5	$.000^{0}$	$.000^{3}$
			10	2.5	$.000^{0}$	$.000^{5}$

Table II (continued)

T °K	R Ω	$\frac{dR}{dT}$ Ω/°K	i μ amp	δR Ω	δT °K corresponding to noise	δT °K corresponding to δR
.5	3600	22000	.1	0	$.000^{5}$	0
			.15	1	$.000^{3}$	$.000^{0}$
			.3	5	$.000^{1}$	$.000^{2}$
			1	20	$.000^{0}$	.001
.4	8500	77000	.015	20	$.001_{5}$	$.000^{3}$
			.035	90	$.000^{5}$	$.001_{5}$
			.05	120	$.000^{3}$	.003
			.15	250	$.000^{1}$	.020
			1	1500	$.000^{0}$	
.3	32000	580000	.005	200	$.000^{7}$	$.000^{3}$
			.01	800	$.000^{3}$	$.001^{3}$
			.015	1100	$.000^{2}$	.002
			.04	1800	$.000^{1}$	.003
			.13	5000	$.000^{0}$	.008
			1	17000	$.000^{0}$	.030

T = temperature, R = Resistance, i = measuring current, $\delta R = R_0 - R_i$ where R_i is the resistance measured with current i and R_0 is the resistance corresponding to 0 measuring current.

Table III. Characteristics of the Sample Germanium Thermometer

T °K	R Ω	dR/dT Ω/°K	i μ amp	δR Ω	δT °K corresponding to noise	δT °K corresponding to δR
25	9.4	.26	100	0	0.000^{8}	0
			200		$.000^{4}$	
20	10.9	.35	100	0	$.000^{6}$	0
			200		$.000^{3}$	
15	14.1	.59	100	0	$.000^{3}$	0
			200		$.000^{2}$	
10	17.8	1.5	50	0	$.000^{3}$	0
			100	0	$.000^{1}$	0
			200	0	$.000^{0}$	.003
				.005		
6	27.2	3.7	20	0	$.000^{3}$	0
			50	0	$.000^{1}$	0
			100	.005	$.000^{0}$	.001
4	36.9	5.9	10	0	$.000^{8}$	0
			20	0	$.000^{4}$	0
			50	.005	$.000^{2}$	.001
2	58.5	20	10	0	$.000^{2}$	0
			20	.01	$.000^{1}$	$.000^{5}$
1	98.5	86	2	0	$.000^{5}$	0
			5	0	$.000^{2}$	0
			10	.03	$.000^{1}$	$.000^{3}$
			20	.09	$.000^{0}$	.001
.7	137	200	2	0	$.000^{5}$	0
			5	.1	$.000^{2}$	$.000^{5}$
.5	199	450	1	0	$.000^{4}$	0
			2	.03	$.000^{2}$	$.000^{1}$
			5	.4	$.000^{1}$	.001
.4	268	900	1	0	$.000^{5}$	0
			2	.3	$.000^{2}$	$.000^{3}$
.3	406	2100	1	0	$.000^{2}$	0
			2	2	$.000^{1}$	.001

Table III. (Continued)

T = temperature, R = resistance, i = measuring current, $\delta R = R_0 - R_i$ where R_i is the resistance measured with current i and R_o is the resistance corresponding to 0 measuring current.

detector in these experiments is essentially the minimum expected from the circuit resistance. For these reasons the thermometers have useful sensitivities over the entire 0.25° to 25°K range. A second important advantage of germanium resistance thermometers over carbon thermometers, and one that is essential to the calibration procedure employed here, stems from the fact that their resistance remains unchanged when they are warmed and then re-cooled.

E. Heat Capacity of Copper

We undertook heat capacity measurements on copper primarily to examine the performance of our calorimeter and the reliability of our temperature scale between 4° and 10°K. The measurements were made on a 900 gram sample of 99.999% pure copper obtained from the American Smelting and Refining Company, South Plainfield, New Jersey.

A plot of C/T versus T^2 for $T < 2°K$, Fig. 6, was used to determine the parameters γ and Θ_o in the equations

$$C = \gamma T + C_\ell \qquad (6)$$

$$C_\ell = \frac{12}{5} \Pi^4 R\left(\frac{T}{\Theta}\right)^3 \qquad (7)$$

$$= \frac{12}{5} \Pi^4 R\left(\frac{T}{\Theta_o}\right)^3 + BT^5 + \ldots\ldots \qquad (8)$$

C_ℓ is the lattice heat capacity which is often characterized by defining a temperature Θ as in Eq. (7). Θ_0 is the limiting value of Θ at $T = 0$. The resulting values are $\gamma = 0.698$ mJ mole^{-1} deg^{-2} and $\Theta_0 = 342°K$, in good agreement with other published values.[16,17]

The measurements above 2°K are shown in Fig. 7 as a plot of Θ versus T. For comparison smoothed Θ obtained by Martin et al.[18] are also shown. The agreement between the two sets of data is well within the combined precision. This fact and the smooth variation of Θ with temperature in the 4° to 10°K region support the validity of our temperature scale in that range.

3. Measurements on Niobium

A cylindrical sample of single crystalline niobium, 1/2" in diameter and 4" long, was obtained from the Materials Research Corporation, Orangeburg, New York. It was triple zone refined with total impurities less than 80 parts per million. Table IV gives the abundance of the various impurities.

The width of the superconducting transition is 0.015°K (see Fig. 8) which is an evidence of the high sample quality.

For the heat capacity measurements the niobium sample was placed in a sample holder made of a minimum amount of copper. The sample germanium thermometer and the heater were attached by G. E. 7031 varnish to the holder. The heat capacity of the empty holder was found to be

$$0.0738T + 0.00959T^3 - 0.305\times10^{-5}T^5 + \frac{0.802}{T^2} \times 10^{-3} \text{ mJ/mole deg}$$

The heat capacity of the niobium sample was determined by subtracting the heat capacity of the empty holder from the total heat capacity.

The superconducting state measurements were made first. The earth's field was reduced by a factor 10 by placing a piece of μ metal around the dewars. The sample was never exposed to a magnetic field during or prior to the superconducting state measurements. The normal state points were taken with the magnet current at 5 and 7 amps which corresponds to a minimum of 2000 and 2500 Oe field on the sample. The mixed state points were taken with the magnet current at 1.2 and 2.4 amps which corresponds respectively to a minimum 500 and 1000 Oe field on the sample. During the mixed state points the sample was always cooled from above the transition temperature in zero field. The field was applied while the sample was at the lowest temperature.

TABLE IV

IMPURITIES IN THE NIOBIUM SAMPLE

Impurity	Abundance
Interstitial (C, O, N, H)	Less than 10 PPM (parts per million)
Fe	ND (non-detectable)
Cu	ND
Mg	ND
Mo	Less than 10 PPM
Si	Less than 20 PPM
Ta	Less than 35 PPM
Va	ND

4. Analysis of Data

The results of the heat capacity measurements on normal, superconducting, and mixed states of niobium are plotted as C/T versus T^2 for $0<T<10°K$ in Fig. 9. The analysis of the data for each state will now be presented.

A. Normal State

The normal state heat capacity C_n at low temperatures can be represented by an equation of the form

$$C_n = C_{nuc} + \gamma T + C_\ell \tag{9}$$

where

$$C_\ell = \frac{12}{5} \Pi^4 R \left(\frac{T}{\theta}\right)^3 \tag{10}$$

$$= \frac{12}{5} \Pi^4 R \left(\frac{T}{\theta_0}\right)^3 + BT^5 + \ldots\ldots \tag{11}$$

C_ℓ is the lattice heat capacity which is characterized by defining a temperature dependent Debye temperature θ as in Eq. (10). θ_0 is the limiting value of θ at $T = 0°K$. C_{nuc} is the nuclear heat capacity arising from the interaction of the magnetic field with the magnetic moment of the niobium nuclei.

The preliminary values for the parameters γ and θ_o in Eqs. (9-11) were determined from a plot of C_n/T versus $T^2 < 15$ K shown in Fig. 10. Points below $T^2 < 2$ were not considered in determining preliminary values for γ and θ_0, because an upward bend associated with the unquenched superconducting regions and the nuclear term appears. This point will be considered in detail in Section 5.

The final values for γ and θ_o were determined by inspecting a series of plots of $\frac{C_n - \gamma T}{T^3}$ versus T^2 with several choices of γ as shown in

Fig. 11. $\frac{C_n - \gamma T}{T^3}$ is extremely sensitive to the choice of γ; a slightly incorrect choice causes this plot to sharply bend toward plus or minus infinity as $T \to 0$. As seen in Fig. 11, $\gamma = 7.89$ millijoules mole^{-1} degree^{-2} causes the plot to deviate sharply toward minus infinity whereas the choice of $\gamma = 7.81$ millijoules mole^{-1} degree^{-2} causes it to sharply bend in the reverse direction. $\gamma = 7.85$ millijoules mole^{-1} degree^{-2} was taken as the best value.

The intersection of the plot of $\frac{C_n - \gamma T}{T^3}$ versus T^2 with the $\frac{C_n - \gamma T}{T^3}$ axis gives the coefficient of the T^3 term hence the limiting value of the Debye temperature, Θ_0. The initial slope of the same plot gives the coefficient B of the T^5 term. The best values were found to be:

$$\Theta_0 = 277°K$$

$$B = 0.0010 \text{ millijoule mole}^{-1} \text{ degree}^{-6}$$

The higher temperature results are best expressed by a plot of Θ as a function of temperature. Figure 12 shows such a plot for niobium for $0 < T < 25°K$.

B. Superconducting State

The superconducting state heat capacity points are plotted as C/T versus T^2 in Figs. 9 and 13. The results at low temperatures are quite striking. As seen in Fig. 13, the slope does not approach that of the normal state but instead levels off around 1.5°K to a slope of about 0.07 millijoules mole^{-1} degree^{-4} (compared to 0.091 for the normal state). Then, around 0.9°K, it starts to bend again to a slope of about 0.2 millijoules mole^{-1} degree^{-4}.

In their very recent measurements on niobium, van der Hoeven, Jr.

and Keesom[19] observed that the superconducting state heat capacity points when plotted as C/T versus T^2 had a small intercept (0.022 millijoules $mole^{-1}$ $degree^{-2}$) which they attributed to some normal state material left in their sample. We do not believe that the peculiar behavior of the superconducting state heat capacity that we observed is due to any normal state material being left in the sample during the measurements. Before the superconducting state measurements the sample was never exposed to a magnetic field; even the earth's field was reduced by a factor of 10. It is more reasonable to think that either the lattice heat capacity of the superconducting state is different from that of the normal state, or, if the lattice contributions are assumed to be the same in both states, then the electronic heat capacity of the superconducting state is not a single exponential term. In analyzing the data, we will choose the second alternative for reasons discussed in Section 5.

The behavior of C_{es} is spectacular, as shown in Fig. 14. Here we plot the log of $C_{es}/\gamma T_c$ which was obtained by subtracting the normal state lattice heat capacity from the total superconducting state heat capacity as a function of T_c/T, T_c being the superconducting transition temperature. The results above 1.5°K can be expressed as

$$\frac{C_{es}}{\gamma T_c} = 7.85 \exp\left(-1.49 \frac{T_c}{T}\right)$$

which is in fair agreement with the BCS theory. Points below 1.3K, fit to an expression of the form

$$\frac{C_{es}}{\gamma T_c} = 2.6\times10^{-3} \exp\left(-0.0525 \frac{T_c}{T}\right)$$

So, the electronic heat capacity of the superconducting state seems to

be best represented as

$$\frac{C_{es}}{\gamma T_c} = 7.85 \exp(-1.49 \frac{T_c}{T}) + 2.6\text{X}10^{-3} \exp(-0.0525 \frac{T_c}{T})$$

C. Mixed State

The mixed state heat capacity points taken with 500 Oe and with 1000 Oe are shown in Fig. 9.* There is no pattern to the points taken with 1000 Oe possibly because of the inhomogeneity of the field. This is in contrast with the observations of Keesom and Radebaugh[20] who found that the mixed heat capacity (C_m) of vanadium at low temperatures fit an equation of the form

$$C_m = 8.8\ T + 1.04\ T^3 \text{ millijoules/mole degree}$$

The points taken with 500 Oe fall on almost the same curve as the superconducting state points up to 3°K. Then, however, they sharply rise, go through a peak, and fall on to the normal state points above 7°K.

D. Comparison With Other Measurements

Prior to our heat capacity measurements on niobium, other measurements had been done, two by Boorse and collaborators[5,21] and one by Chou et al.[22] A few months ago two additional measurements were reported, one by van der Hoeven, Jr. and Keesom (HK)[19] and the other by Leupold and Boorse (LB).[23] The results of these measurements are given together with our results in Table V. Our values for γ and Θ_0 agree well with the recent work of HK and LB. It is interesting to note here that both HK and LB interpret the upward bend in their C_n/T versus T^2 plots as a consequence of a sharp change

* The field values given are the minimum values on the sample.

TABLE V

SUMMARY OF CALORIMETRIC AND RELATED DATA FOR NIOBIUM

Measurement	Range °K	Transition Temp. °K	γ mJ/mole deg^2	Θ_o °K
Calorimetric Brown et al.[21]	2.5-11	8.70 ± .10	8.52	252
Calorimetric Hirshfeld et al.[5]	1.1-11.5	9.09 ± .08	7.38	241
Calorimetric Chou et al.[22]	1.5-30	9.07 - 9.17	7.52	256-320
Calorimetric Leupold and Boorse[23]	.4-10	9.0 - 9.3	7.80	275
Calorimetric van der Hoeven Jr. & Keesom[19]	.4-3	-	7.79	275
Calorimetric This work	.25-25	9.264±0.008	7.85	277
Elastic Constants Alers & Waldorf[24]	-	-	-	277

in the Debye temperature. A fairly sharp upward bend also exists in our data but it is not so sharp as to suggest the assumption that the Debye temperature changes abruptly. The upward bend in our plot of C_n/T versus T^2 starts around $T^2 = 6$, around $T^2 = 10$ the points are about 1.5% higher than the line $7.85\ T + 0.0915\ T^3$ millijoules/mole degree and around $T^2 = 15$ about 2% higher. We believe that this bend is simply due to the T^5 term which becomes appreciable around 3°K.

Above 1.5°K the parameters for the superconducting state electronic heat capacity (C_{es}) agree with those of LB and HK. Below 1.3°K, however, we find that

$$\frac{C_{es}}{\gamma T_c} = 2.6\times10^{-3} \exp(-0.0525 \frac{T_c}{T})$$

The energy gap is estimated from the heat capacities above 1.5°K as

$$\frac{1.49}{1.44} \times 3.50\ kT_c = 3.62\ kT_c$$

and below 1.3°K as

$$\frac{0.053}{1.44} \times 3.50\ kT_c = .13\ kT_c$$

For comparison the energy gap values determined by other methods are given in Table VI.

The limiting value for the Debye temperature calculated from the elastic constant measurements[24] is in excellent agreement with our value of 277°K.

The discrepancy between the results of the recent measurements and those of the earlier experiments stems primarily from the poor quality of the samples used in the earlier measurements. For example, the sample which Boorse and collaborators used in their 1953 measurements was only 99.8% pure compared to the 99.992% purity now available. The precision of these

TABLE VI

ENERGY GAP FOR NIOBIUM AT 0°K

IN UNITS OF kT_c

MEASUREMENT	GAP
Richards and Tinkham[43] (IR absorption)	2.8 ± 0.3
Giaever[44] (Tunneling)	3.6
Sherril and Edwards[45] (Tunneling)	3.59
Townsend and Sutton[46] (Tunneling)	3.84 ± 0.06
Mendelssohn[47] (Thermal Conductivity)	3.8 ± 0.2
Dobbs and Perez[48] (Ultrasonic)	3.77 (for 100 direction) 3.74 (for 111 direction) 3.65 (for 110 direction)
Levy et al[49] (Ultrasonic)	3.7

earlier measurements was not good either as illustrated by Chou et al. reporting in their 1958 paper that the limiting value of θ was somewhere between 256° and 320°K.

A good criterion for determining sample quality is the value of the transition temperature and the width of the transition. It should be noted that the transition temperatures reported in the earlier measurements are considerably lower than the recent values. The width of the transition reported by Leupold and Boorse[23] in their latest measurements is 300 millidegrees compared to 15 millidegrees observed in our measurements. We, therefore, believe that the values reported in this thesis are the best available calorimetric parameters on niobium.

5. DISCUSSION

At the lowest temperatures, the points taken in 2000 and 2500 Oe magnetic fields do not follow a straight line when plotted as C/T vs T^2, as would be expected for the lattice and electronic heat capacities of a normal metal. As T decreases below 1.5°K with H = 2000 Oe, or below 1°K with H = 2500 Oe, the points rise above the expected straight line (an indication of this trend can be seen in Fig. 9) and then bend downward. At the lowest temperatures the points taken in 2500 Oe are higher than those in 2000 Oe. It appears that the deviations from the expected straight line are produced by two effects: a heat capacity associated with unquenched superconductivity in some regions of the sample, and a nuclear heat capacity associated with the splitting of the nuclear levels by the external field, which is important only at the lowest temperatures. To see whether this is indeed the case, we estimated the nuclear term using the expression

$$C_{nuc} = \frac{1}{3}\,\frac{I+1}{I}\,\left(\frac{\mu H}{kT}\right)^2 R$$

where I is the nuclear spin (for niobium it is 9/2), μ is the nuclear magnetic moment, H is the magnetic field, k is the Boltzman constant, and R is the gas constant.* Subtracting the estimated nuclear term from the total heat capacity, we found that the resultant heat capacity with H = 2000 Oe shows a larger peak than that with H = 2500 Oe - in accordance with our picture that the rest of the excess heat capacity is associated with unquenched superconducting regions.

---

* This expression holds true at temperatures where kT is much greater than the spacing of the nuclear energy levels.

We undertook the mixed state measurements on niobium in order to check the validity of a proposal by Rosenblum and Cardona.[25] They had proposed that in a Type II superconductor (of which niobium is believed to be an example) the intermediate state contains normal regions and a fraction, H/H_{C_2} (where H is the applied field and H_{C_2} is the upper critical field) of the sample is made up of such normal regions. Since, at very low temperatures, H_{C_2} is fairly constant one expects to see a linear term in the heat capacity of the intermediate state. The magnitude of the linear term should be $\gamma(H/H_{C_2})$. Contrary to the observations of Keesom and Radebough who do report a linear term for the intermediate state of vanadium, we found no pattern in the heat capacity points of niobium taken with 1000 Oe.

The points taken with 500 Oe which is below the lower critical field follow the same curve as the superconducting state points up to 3°K, then they begin to deviate upwards, and around 5°K a fairly sharp peak appears. The width of this peak is about 2°K. McConville and Serin[26] also observed such a peak in a lower magnetic field which they interpreted as an evidence of first order transition supporting P. M. Marcus'[27] calculations. Our observation can also be interpreted as a first order transition; the ratherlarge width of the transition being due to the unhomogeneity of the magnetic field over the sample. Since we were primarily interested in the superconducting and normal state heat capacities, we made no effort to get a homogeneous field over the sample volume. McConville and Serin also reported a sudden jump in the heat capacity around 7.2°K which we did not observe. This, however, might be due to the fact that we did not use sufficiently small temperature increments.

The limiting value for the Debye temperature determined from the

normal state heat capacities (277°K) is in perfect agreement with that calculated from the elastic constant measurements (277°K). This is in violation with the theory of G. M. Eliashberg[28] who predicted a contribution of the form $T^3 \log T$ to the normal state heat capacity arising from the electron phonon interaction.

The behavior of the superconducting state heat capacity, C_s, is anomalous in the sense that it is impossible to express it at low temperatures as

$$C_s \doteq a\gamma\, T_c \exp(-b\, \frac{T_c}{T}) + \alpha\, T^3$$

where $a\gamma T_c \exp(-b\, \frac{T_c}{T})$ is the electronic heat capacity predicted by the BCS theory and αT^3 is the lattice heat capacity. As seen in Fig. 13, C_s/T versus T^2, C_s, instead of approaching a limiting value equal to the normal state lattice heat capacity, levels off around $T^2 = 2$ and then bends down again around $T^2 = 0.6$. Although this anomalous behavior does not allow a simple comparison of the lattice heat capacities of the normal and superconducting states, the total superconducting state heat capacity definitely does not fall below the normal state lattice term as it does in indium - the only other superconductor for which the experimental evidence clearly indicates that $C_{\ell s} \ngeq C_{\ell n}$.

In connection with the anomalous behavior in niobium three possibilities that might be considered are: (1) Some normal state material remains in the sample during the superconducting state measurements; (2) The lattice heat capacities for the normal and superconducting states ($C_{\ell n}$ and $C_{\ell s}$ respectively) are not the same; (3) $C_{\ell n} = C_{\ell s}$, but the superconducting state electronic heat capacity, C_{es}, is not expressible as a single exponential term as predicted by a single energy gap model of

superconductors. It is also conceivable that the superconducting state heat capacity is not a sum of separable electronic and lattice terms, but there is no theoretical model worked out with which we could have compared our data, and therefore, this possibility will not be considered.

We discarded the probability that there might have been some normal state material left during the superconducting state measurements because there is no reason why any normal material should be left when the sample is cooled without being exposed to a field. Furthermore, if there were some normal material left than one would expect the limiting slope of C_s/T to become parallel to the slope of C_n/T as had been observed for lead,[3] mercury,[3] indium,[1] and tin[1] in measurements made in this laboratory using an adiabatic demagnetization calorimeter. For niobium the limiting slope of C_s/T does not become parallel to that of C_n/T.

If we attempt to interpret the niobium anomaly as a result of unequal lattice heat capacities then we have to conclude that $C_{\ell s}$ does not have a T^3 dependence. This is clearly seen in Fig. 13, C_s/T versus T^2, where the slope is not constant at temperatures for which the BCS theory gives a negligible C_{es}. The niobium anomaly then is of a different sort than that of indium for which the lattice terms appear to be unequal although both vary as T^3. (It should also be remarked that the indium anomaly is not definitely due to a difference between $C_{\ell s}$ and $C_{\ell n}$, and none of the other superconductors investigated in this laboratory, lead, tin and mercury, has shown any indication that $C_{\ell s} \neq C_{\ell n}$. Thus, if the lattice heat capacities are assumed to be unequal, we are forced to conclude that $C_{\ell s}$ has a complicated temperature dependence for which there is no precedent. Since no superconductor shows a lattice heat capacity anomaly except indium (and even that is not certain) it is more reasonable to interpret the niobium

anomaly as a result of a superconducting electronic heat capacity which is not expressible as a single exponential term.

If it is assumed that $C_{\ell n} = C_{\ell s}$ then the electronic heat capacity of the superconducting state is best expressed as

$$\frac{C_{es}}{\gamma T_c} = 7.85 \exp(-1.49 \frac{T_c}{T}) + 2.6\text{X}10^{-3} \exp(0.0525 \frac{T_c}{T})$$

which implies that the energy gap in niobium is highly anisotropic. First experimental evidence for the anisotropy of the energy gap came from the heat capacity measurements of Goodman (1957, 1958),[29,30] Zavaritskii (1958),[31] and Phillips (1959).[32] At low temperatures they observed a slight upward deviation from a straight line in the plot of log $(C_{es}/\gamma T_c)$ versus T_c/T. The deviations, however, were small and not the same in measurements made in different laboratories. In 1959, Cooper[33] pointed out that this deviation could be a result of the anisotropy of the energy gap. In subsequent years ultrasonic attenuation[34,35,36] and IR absorption experiments[37] have clearly established that the energy gap is anisotropic. None of the earlier calorimetric measurements indicated a gap so anisotropic as that suggested by the measurements reported here, but they were all made on non-transition metals. The possibility of enhanced energy gap anisotropy in transition metals has been predicted by Garland[38] in connection with his theory of the isotope effect in transition metals. Very recent measurements by Y. L. Shen[39] on vanadium and tantalum show that the energy gap in these metals is also highly anisotropic. The anisotropy of the gap, however, is sensitive to impurities and, as has been shown by Anderson,[40] is gradually wiped out by the impurity scattering centers as the sample becomes impure. The gap becomes completely

isotropic when

$$\frac{h}{2\,\Pi}\,\frac{V_o}{2\epsilon(o)} \approx \xi_o$$

where V_o = the electron mean free path, $2\epsilon(o)$ = the BCS energy gap, and ξ_o = the coherence length for the pure material. Anderson's theory has been supported by the experiments of Serin, Lynton and collaboratores[41,42] who studied the superconducting properties of dilute alloys of various solutes in tin, indium, and aluminum. Apparently our niobium sample is pure enough to show a strong gap anisotropy as is indicated by the electronic heat capacity of the superconducting state.

In conclusion we may state that the very low temperature heat capacity of superconducting niobium is anomalous and the anomaly is best understood in terms of extreme energy gap anisotropy. This result can be taken as supporting Garland's treatment of superconductivity in transition metals.

ACKNOWLEDGMENTS

I would like to express my gratitude to Professor Norman E. Phillips for his guidance, unfailing interest, and friendship.

I would also like to thank Y. L. Shen who has helped in calculating many of these results.

This work was performed under the auspices of the United States Atomic Energy Commission.

PART II

REFERENCES

1. H. R. O'Neal and N. E. Phillips, Phys. Rev. (in press); H. R. O'Neal (Ph.D. Thesis) University of California, Berkeley (1963).
2. C. A. Bryant and P. H. Keesom, Phys. Rev. 123, 491 (1961).
3. N. E. Phillips, M. H. Lambert and W. R. Gardner, Rev. Mod. Physics, 36, 131 (1964).
4. P. H. Keesom and B. J. C. van der Hoeven, Phys. Letters 3, 360 (1963).
5. A. T. Hirshfeld, H. A. Leupold, and H. A. Boorse, Phys. Rev. 127, 150 (1962).
6. H. S. Sommers, Jr., Rev. Sci. Instruments 25, 793 (1954).
7. F. E. Hoare, J. C. Mathews and B. Yates, Proc. Phys. Soc. B 68, 388 (1955).
8. E. Ambler and R. P. Hudson, J. Res. Nat. Bur. Stand. 56, 99 (1956).
9. E. Ambler and R. P. Hudson, J. Res. Nat. Bur. Stand. 57, 23 (1956).
10. H. H. Plumb, M. H. Edlow and G. Cataland, Progress in Refrigeration Science and Technology, Vol. I, (Pergamon Press, London, 1960) p. 184.
11. R. Berman and C. F. Mate, Nature 182, 1661 (1958).
12. R. A. Erickson, L. D. Roberts and J. W. T. Dabbs, Rev. Sci, Instruments 25, 1178 (1954).
13. J. M. Daniels and F. N. K. Robinson, Phil. Mag. 44, 630 (1953).
14. C. A. Bailey, Proc. Phys. Soc., 83, 369 (1964).
15. J. R. Clement and E. H. Quinnell, Rev. Sci. Instruments 23, 213 (1952).
16. N. E. Phillips, Phys. Rev. 134 A385 (1964).
17. R. R. Hake, Phys. Rev. 123, 1986 (1961).
18. J. P. Franck, F. D. Manchester and D. L. Martin, Proc. Roy. Soc. A263, 494 (1961).

19. B. J. C. van der Hoeven, and P. H. Keesom, Phys. Rev. 134 A1320 (1964).

20. P. H. Keesom and R. Radebaugh, Phys. Rev. Letters 13, 685 (1964).

21. A. Brown, M. W. Zemansky and H. A. Boorse, Phys. Rev. 92, 52 (1953).

22. C. Chou, D. White and H. L. Johnston, Phys. Rev. 109, 788 (1958).

23. H. A. Leupold and H. A. Boorse, Phys. Rev. 134, A1322 (1964).

24. G. A. Alers and D. L. Walsdorf, Phys. Rev. Letters 6, 677 (1961).

25. B. Rosenblum and M. Cardona, Phys. Rev. Letters 12, 657 (1964).

26. T. McConville and B. Serin, Phys. Rev. Letters 13, 365 (1964).

27. P. M. Marcus, Bull. Am. Phys. Soc 9, 438 (1964).

28. G. M. Eliashberg, Zh. Eksperim. i Teor. Fiz. 43, 1005 (1962); [Engl. Trans.: Soviet Phys.-JETP 16, 780 (1963)].

29. B. B. Goodman, C. R. Acad. Sci. 224, 2899 (1957).

30. B. B. Goodman, C. R. Acad. Sci. 246, 3031 (1958).

31. N. V. Zavaritskii, J.E.T.P. USSR 34, 1116 (1958); [Engl. Trans: Soviet Phys. J.E.T.P. 7, 773 (1959)].

32. N. E. Phillips, Phys. Rev. 114, 676 (1959).

33. L. N. Cooper, Phys. Rev. Letters 3, 17 (1959).

34. R. W. Morse, T. Olsen, J. D. Gavenda, Phys. Rev. Letters 3, 15 (1959).

35. R. W. Morse, I.B.M. Jl, 6, 58 (1962).

36. P. O. Bezuglyi, A. A. Galkin, A. P. Karolyuk, J.E.T.P. USSR 36, 1951 (1959); [Engl. Trans.: Sov. Phys., J.E.T.P. 9, 1388].

37. P. L. Richards, Phys. Rev. Letters 7, 412 (1961).

38. J. W. Garland, Jr., Phys. Rev. Letters 11, 114 (1963).

39. Y. L. Shen, (private communication).

40. P. W. Anderson, J. Phys. Chem. Sol., 11, 26 (1959).

41. E. A. Lynton, B. Serin and M. Zucker, J. Phys. Chem. Solids 3, 165 (1959).

42. G. Chanin, E. A. Lynton and B. Serin, Phys. Rev 114, 719 (1959).

43. P. L. Richards and M. Tinkham, Phys. Rev. 119, 575 (1960).

44. I. Giaever, Eighth International Conference on Low Temperature Physics, (Butterworth's Scientific Publications, Ltd., London, 1962).

45. M. D. Sherril and H. H. Edwards, Phys. Rev. Letters 6, 460 (1961).

46. P. Townsend and J. Sutton, Phys. Rev. 128, 591 (1962).

47. K. Mendelssohn, IBM Jl., 6, 27 (1962).

48. E. R. Dobbs and J. M. Perez, International Conference on the Science of Superconductivity, Colgate University, August 1963.

49. M. Levy, R. Kagiwada, and I. Rudnick, Phys. Rev. 132, 2039 (1963).

PART II

FIGURE CAPTIONS

Fig. 1 The calorimeter.

Fig. 2 Heating curves for two typical heat capacity points.

Fig. 3 Schematic drawing of the He^3 system.

Fig. 4 Thermal conductivity of the mechanical switch.

Fig. 5 Salt pill assembly.

Fig. 6 Heat capacity of copper between 0.3° and 2°K.

Fig. 7 Variation of the Debye temperature of copper with temperature.

Fig. 8 Heat capacity of niobium in the transition region.

Fig. 9 Heat capacity of niobium for $0 < T^2 < 100$ - a selection of points for all fields.

Fig. 10 Normal state heat capacity of niobium for $T^2 < 15$.

Fig. 11 Normal state lattice heat capacity of niobium corresponding to several values of γ.

Fig. 12 Variation of the Debye temperature of niobium with temperature.

Fig. 13 Superconducting state heat capacity of niobium for $0 < T^2 < 10$.

Fig. 14 Superconducting electronic heat capacity of niobium.

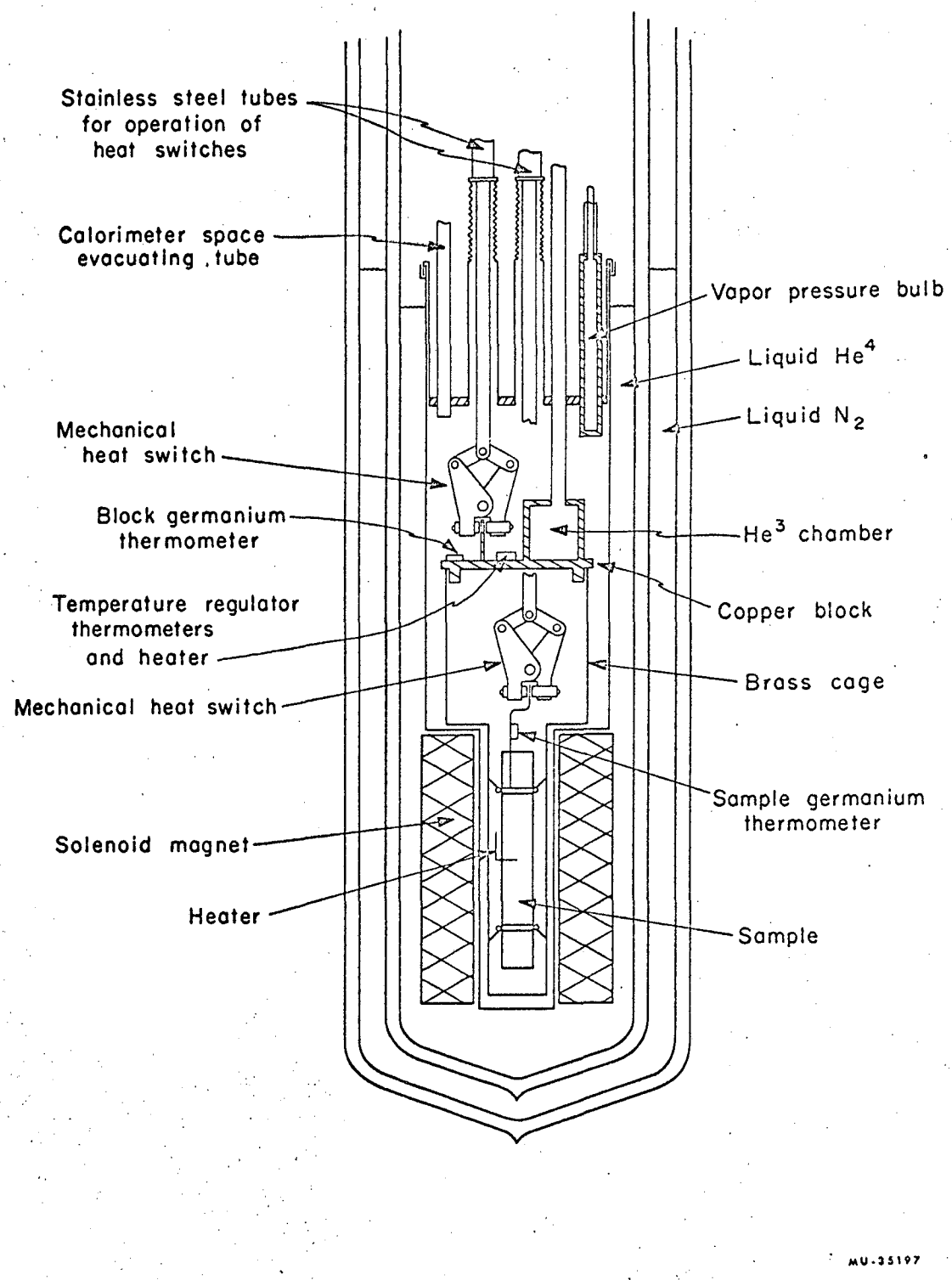
Stainless steel tubes for operation of heat switches
Calorimeter space evacuating tube
Vapor pressure bulb
Liquid He^4
Liquid N_2
Mechanical heat switch
Block germanium thermometer
He^3 chamber
Temperature regulator thermometers and heater
Copper block
Brass cage
Mechanical heat switch
Sample germanium thermometer
Solenoid magnet
Heater
Sample
MU-25197

Figure 1

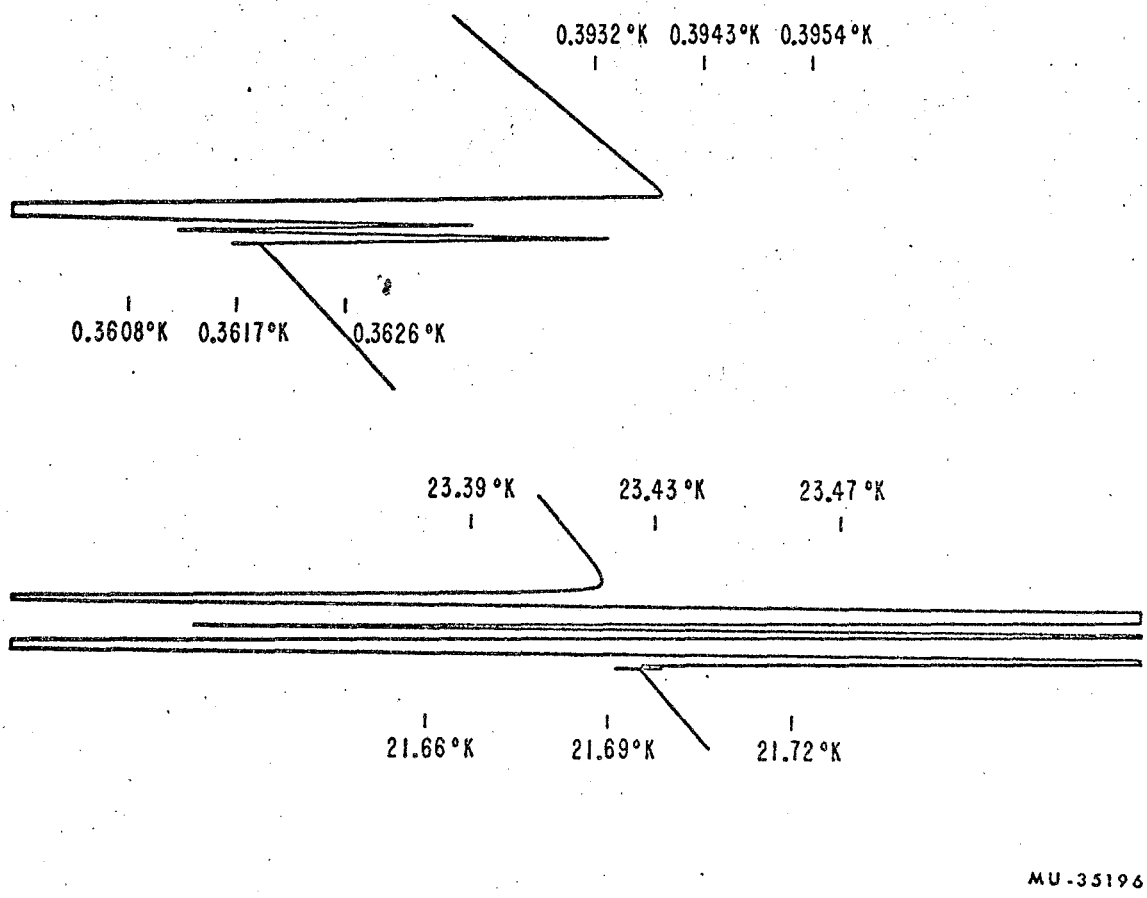
0.3932 °K
0.3943 °K
0.3954 °K
0.3608 °K
0.3617 °K
0.3626 °K
23.39 °K
23.43 °K
23.47 °K
21.66 °K
21.69 °K
21.72 °K
MU-35196

Figure 2

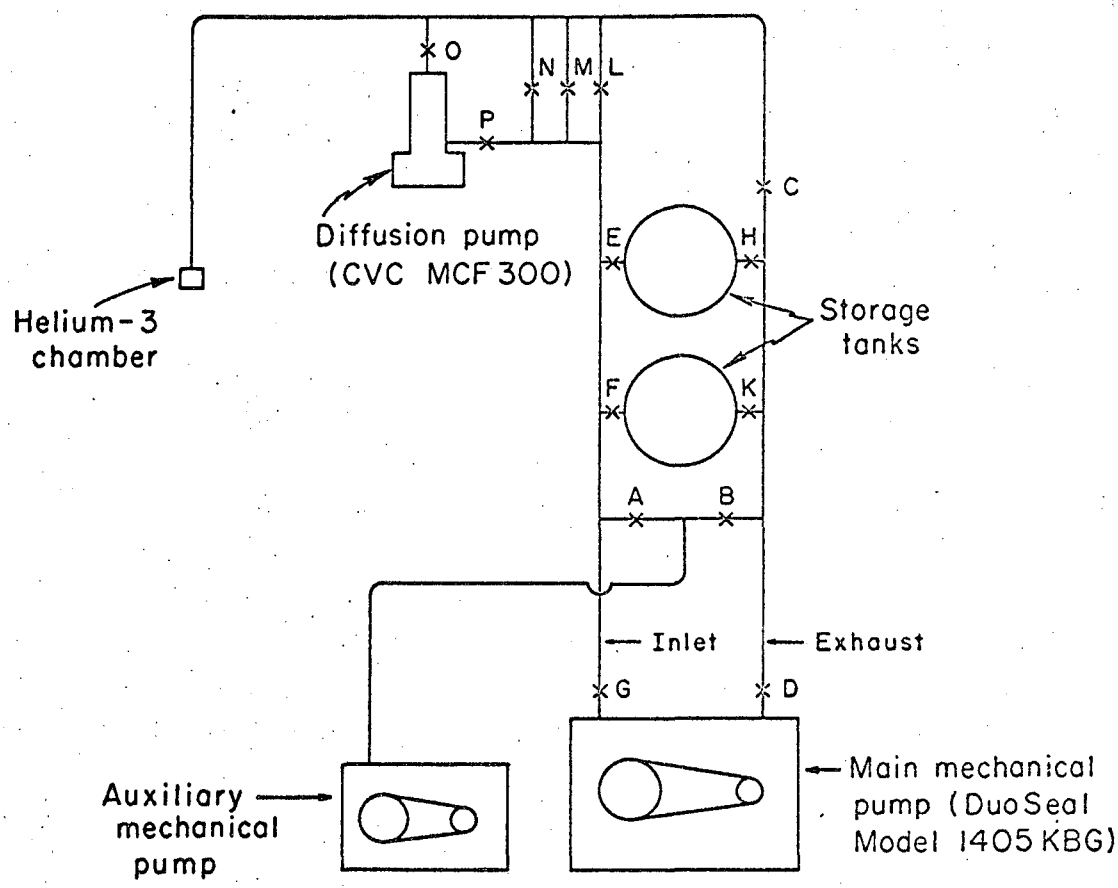

MU-35187

Figure 3

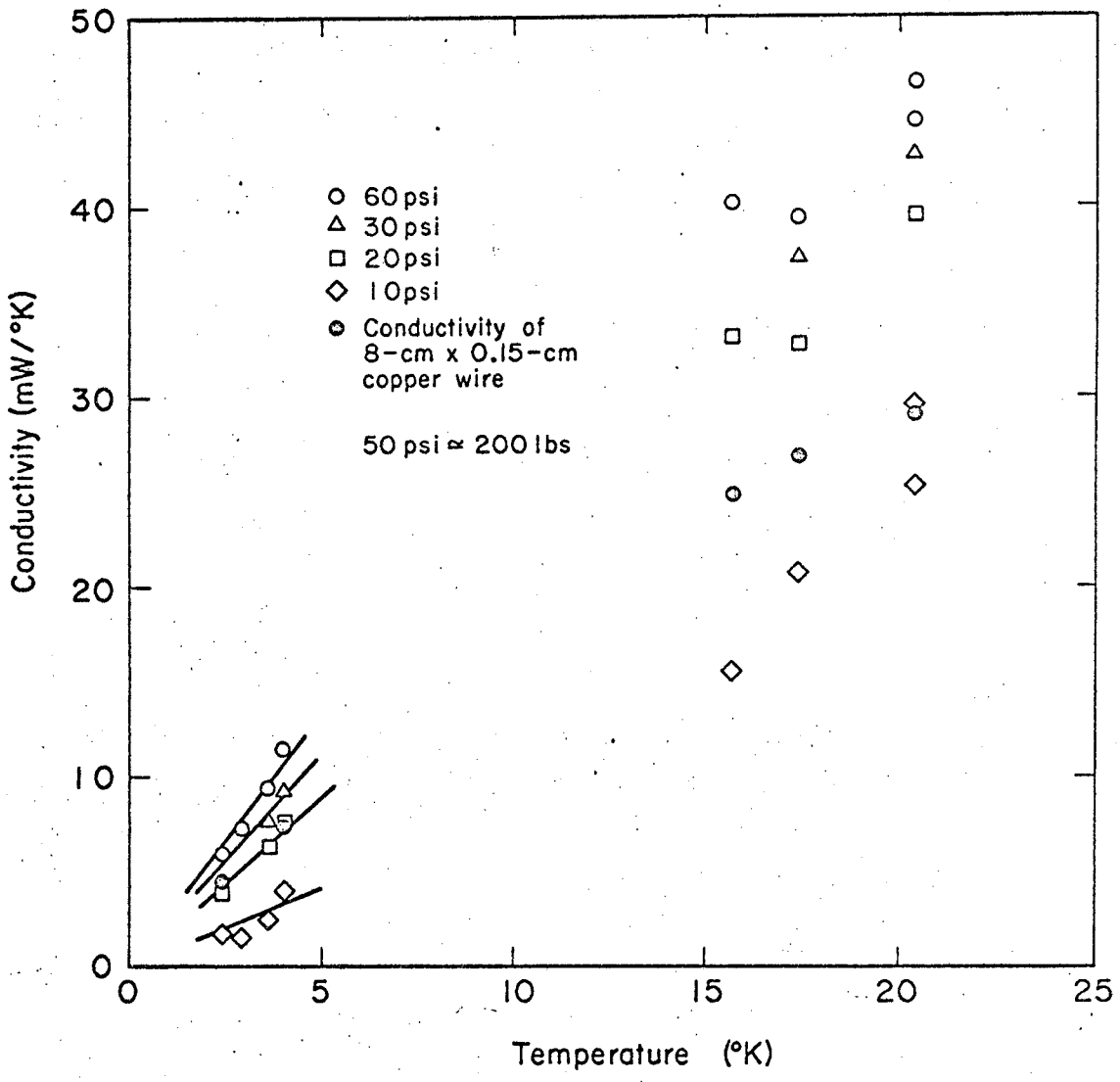

MU-35188

Figure 4

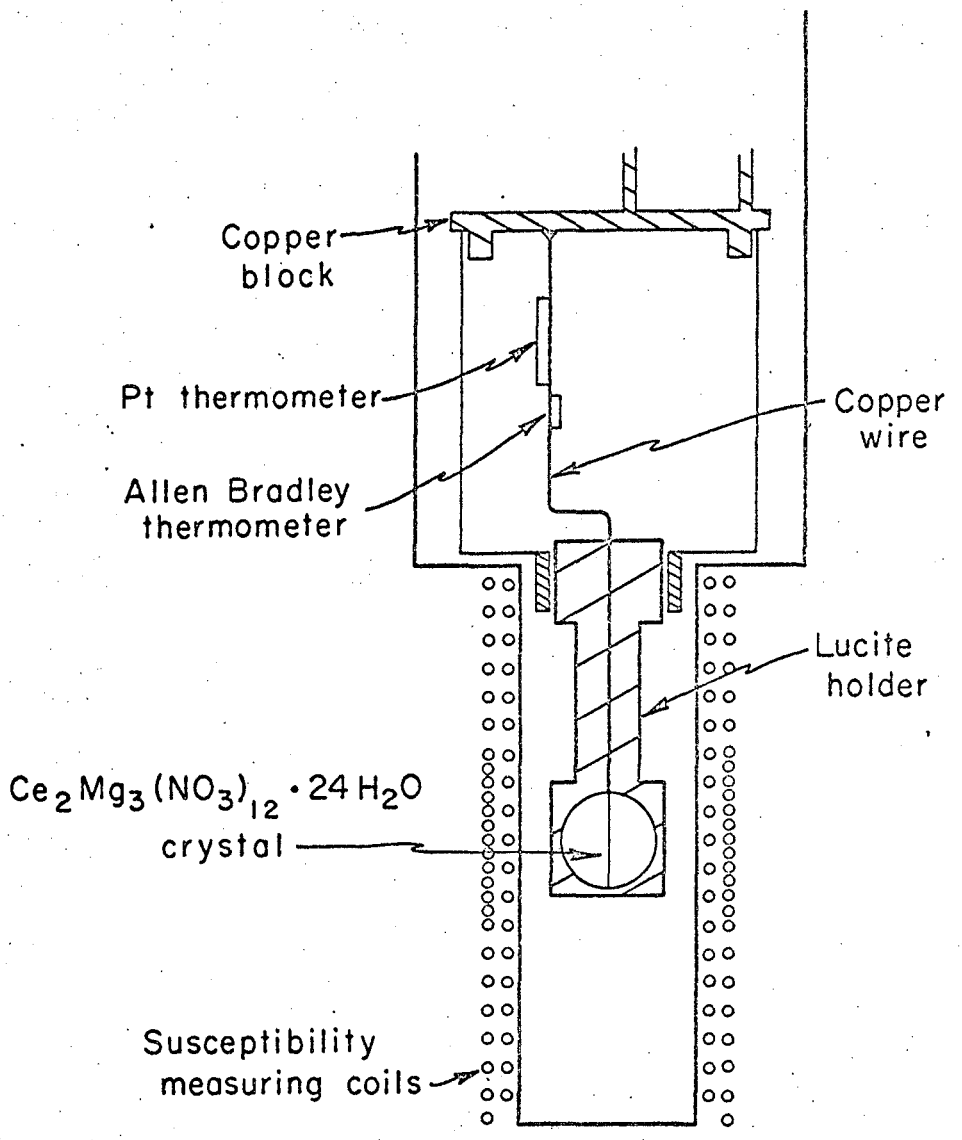

MU-35195

Figure 5

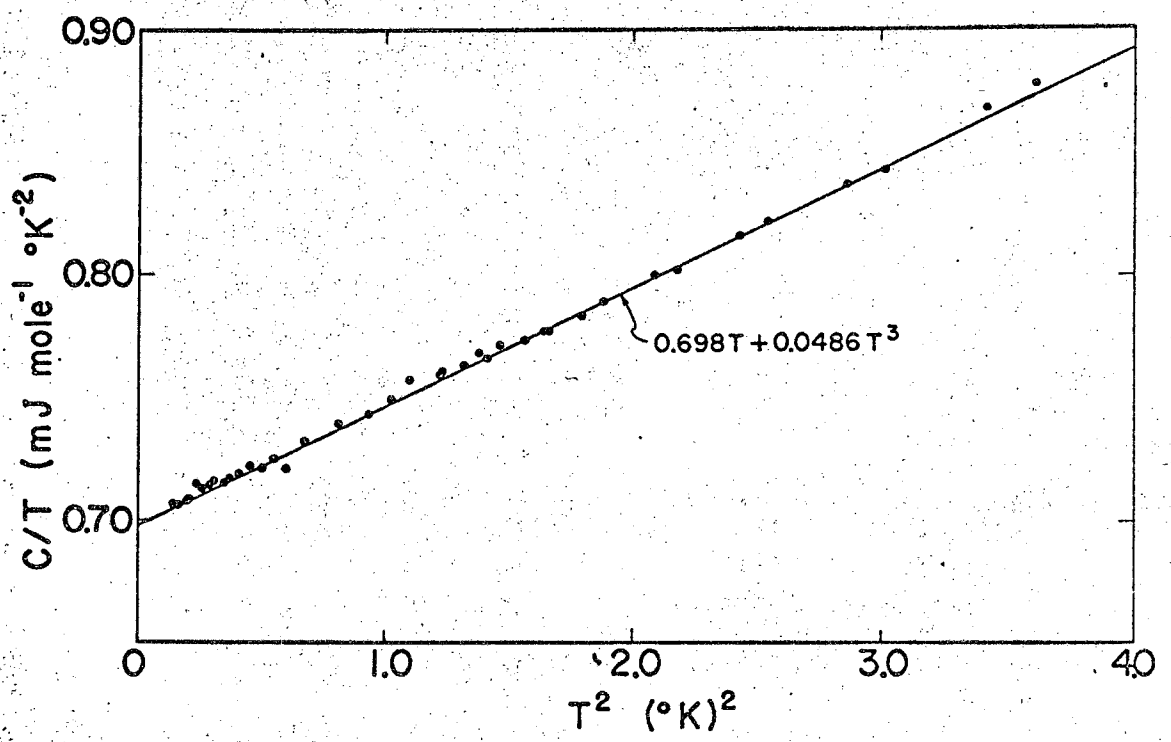

Figure 6

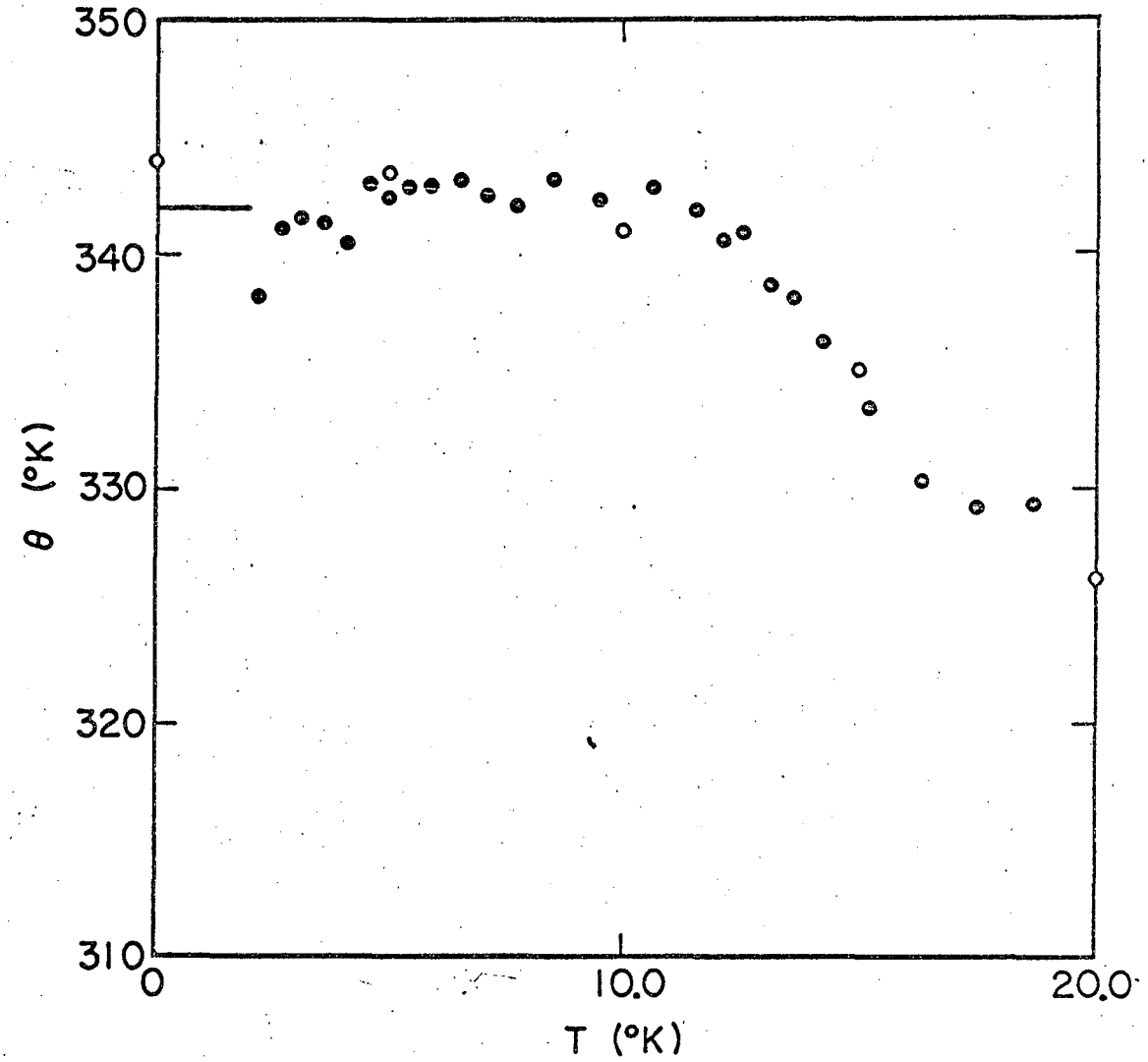

MU-35202

Figure 7

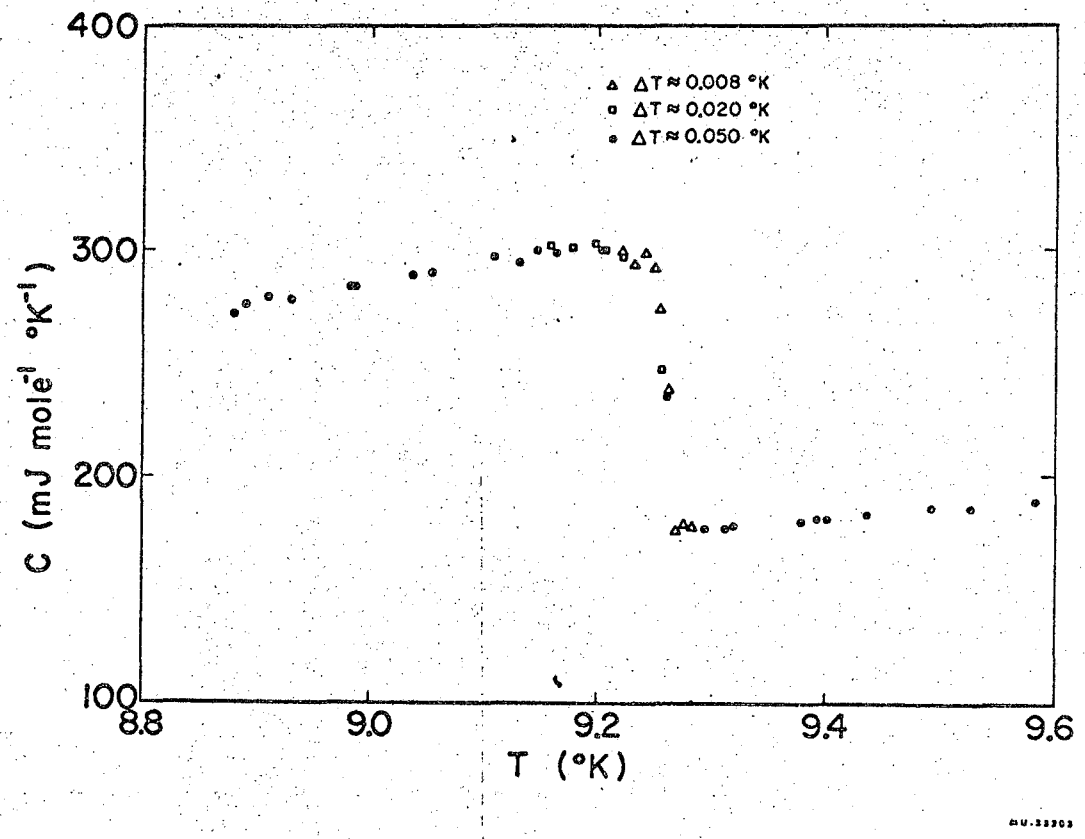
400
300
200
100
8.8
9.0
9.2
9.4
9.6
T (°K)
C (mJ mole⁻¹ °K⁻¹)
△ ΔT ≈ 0.008 °K
□ ΔT ≈ 0.020 °K
● ΔT ≈ 0.050 °K

Figure 8

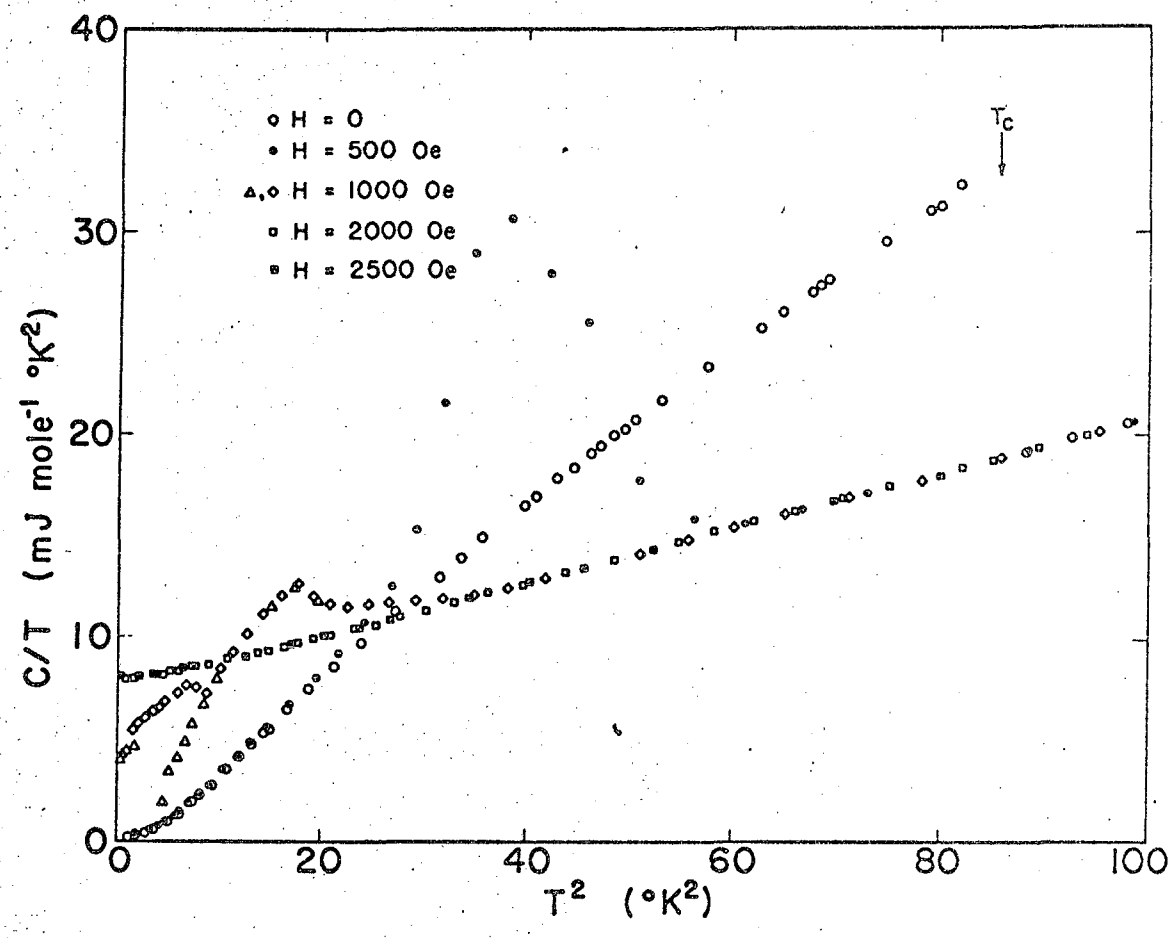
H = 0
H = 500 Oe
H = 1000 Oe
H = 2000 Oe
H = 2500 Oe
T_c
C/T (mJ mole^{-1} °K^2)
T^2 (°K^2)
0
10
20
30
40
0
20
40
60
80
100

Figure 9

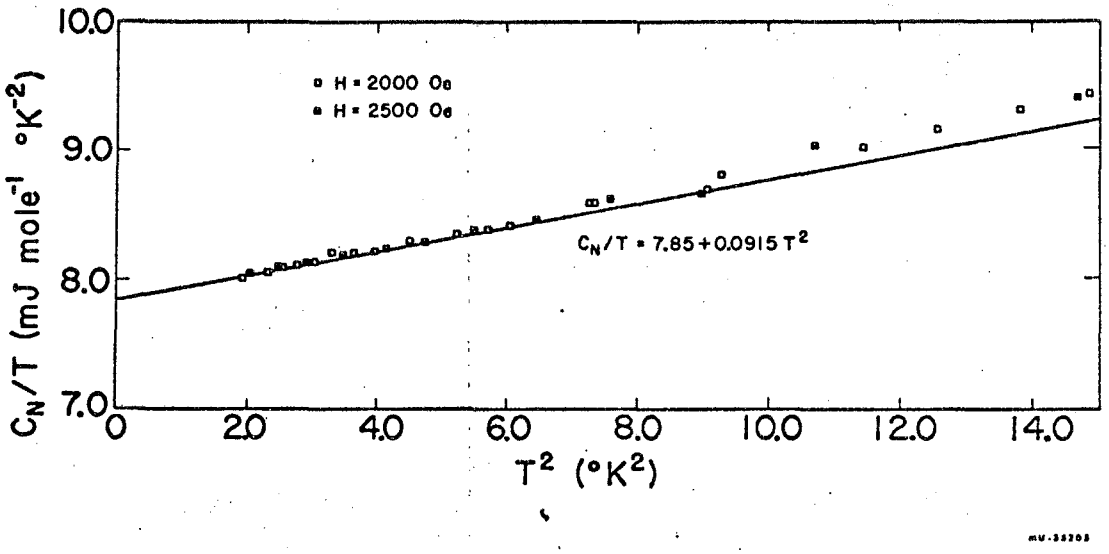
10.0
9.0
8.0
7.0
0
2.0
4.0
6.0
8.0
10.0
12.0
14.0
C_N/T (mJ mole^{-1} °K^{-2})
T^2 (°K^2)
H = 2000 Oe
H = 2500 Oe
$C_N/T = 7.85 + 0.0915\,T^2$

Figure 10

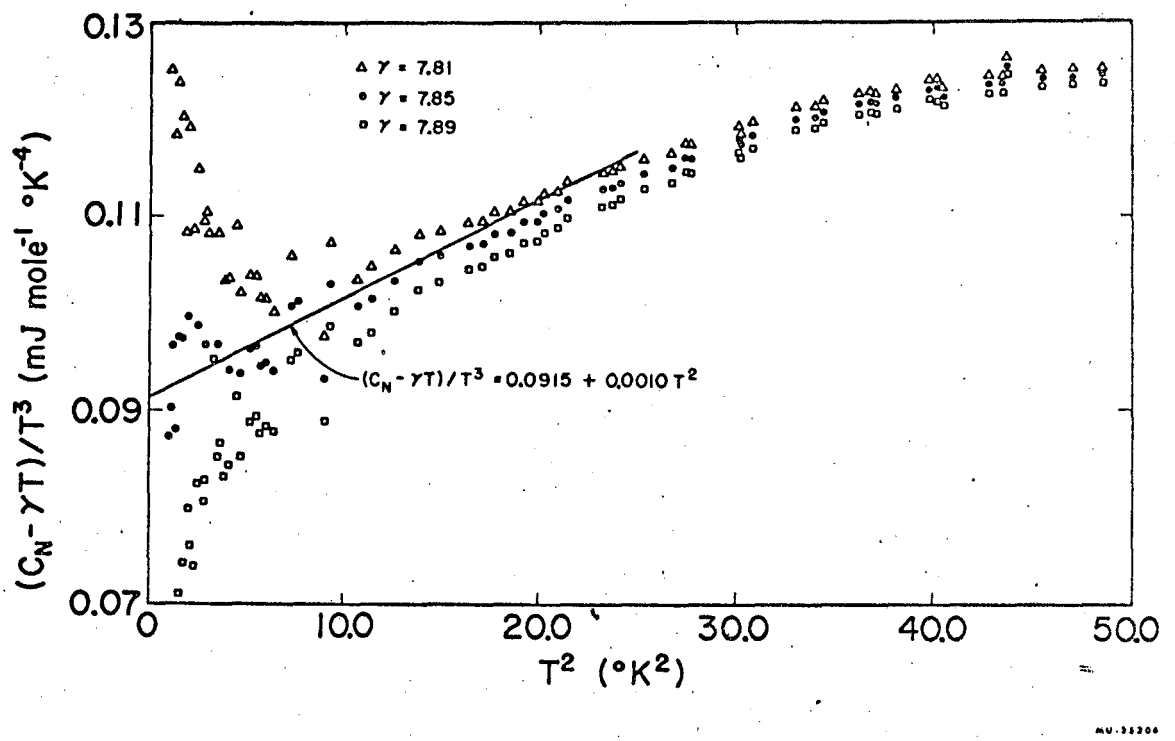
0.13
0.11
0.09
0.07
0
10.0
20.0
30.0
40.0
50.0
T^2 (°K^2)
$(C_N - \gamma T)/T^3$ (mJ mole^{-1} °K^{-4})
△ γ = 7.81
● γ = 7.85
□ γ = 7.89
$(C_N - \gamma T)/T^3 = 0.0915 + 0.0010\,T^2$

Figure 11

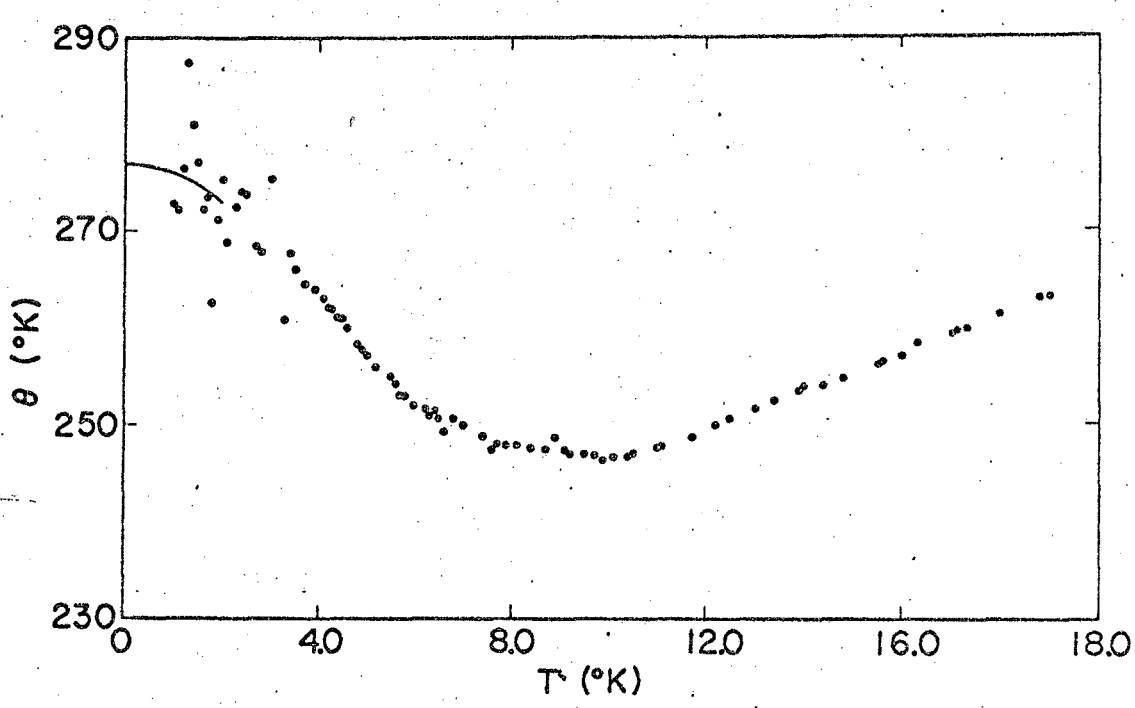

Figure 12

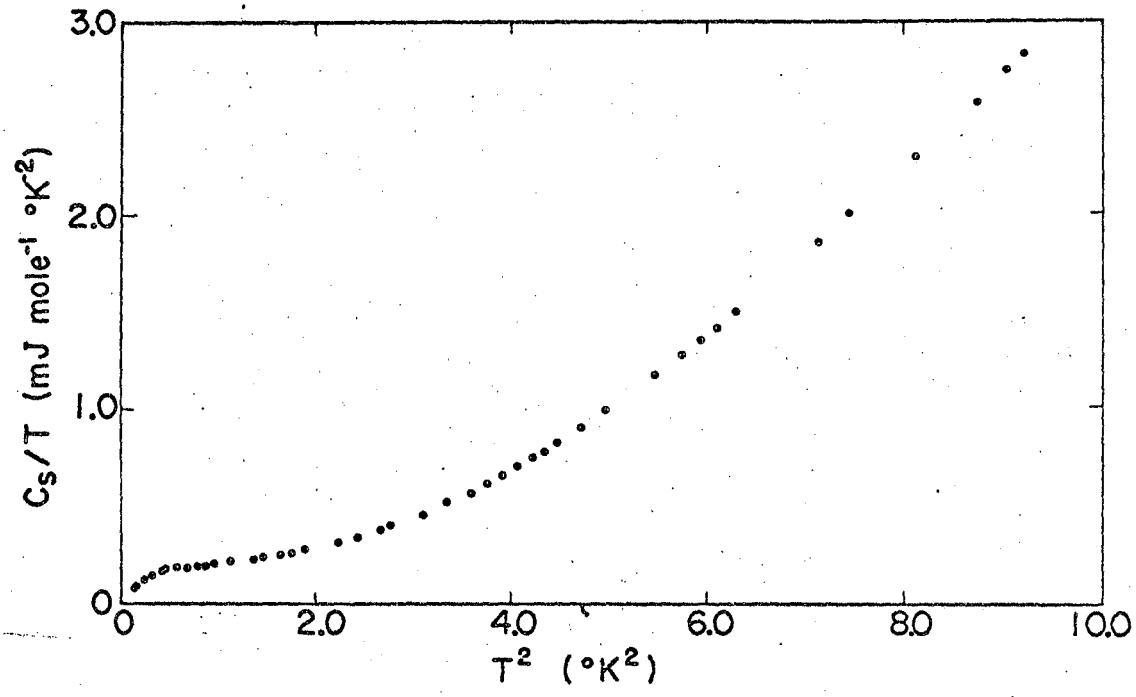

Figure 13

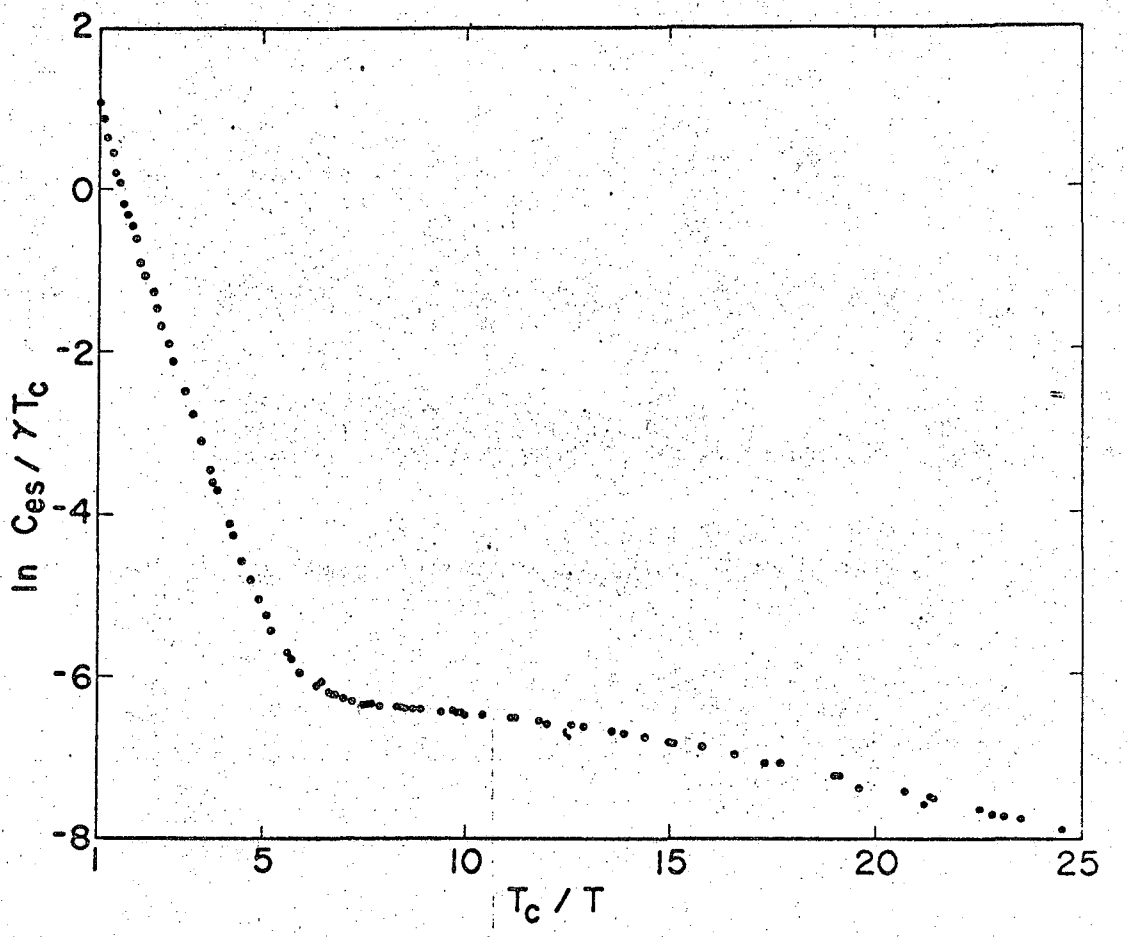

Figure 14

This report was prepared as an account of Government sponsored work. Neither the United States, nor the Commission, nor any person acting on behalf of the Commission:

A. Makes any warranty or representation, expressed or implied, with respect to the accuracy, completeness, or usefulness of the information contained in this report, or that the use of any information, apparatus, method, or process disclosed in this report may not infringe privately owned rights; or

B. Assumes any liabilities with respect to the use of, or for damages resulting from the use of any information, apparatus, method, or process disclosed in this report.
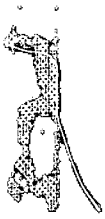
As used in the above, "person acting on behalf of the Commission" includes any employee or contractor of the Commission, or employee of such contractor, to the extent that such employee or contractor of the Commission, or employee of such contractor prepares, disseminates, or provides access to, any information pursuant to his employment or contract with the Commission, or his employment with such contractor.